Report No. FAA-RD-76-45

FLIGHT TESTS OF DIGITAL DATA TRANSMISSION AT VHF

J. R. Juroshek
G. E. Wasson
G. H. Stonehocker

March 1976

Final Report

U.S. DEPARTMENT OF TRANSPORTATION
FEDERAL AVIATION ADMINISTRATION
Systems Research and Development Service
Washington, D.C. 20591

Technical Report Documentation Page

1. Report No.	2. Government Accession No.	3. Recipient's Catalog No.
FAA-RD-76-45		

4. Title and Subtitle	5. Report Date
Flight Tests of Digital Data Transmission at VHF	March 1976
	6. Performing Organization Code: OT/ITS, Division 1
7. Author(s): J. R. Juroshek, G. E. Wasson, G. H. Stonehocker	8. Performing Organization Report No.: DOT-TSC-FAA-76-6
9. Performing Organization Name and Address: U. S. Department of Commerce* Office of Telecommunications Institute for Telecommunication Sciences Boulder, CO 80302	10. Work Unit No. (TRAIS): FA613/R6116
	11. Contract or Grant No.: (RA)76-2 411-0021
12. Sponsoring Agency Name and Address: U. S. Department of Transportation Federal Aviation Administration Systems Research and Development Service Washington, DC 20591	13. Type of Report and Period Covered: Final Report August 1975-January 1976
	14. Sponsoring Agency Code

15. Supplementary Notes

*Interagency Agreement with: U.S. Department of Transportation Transportation Systems Center Kendall Square, Cambridge, MA 02142

16. Abstract

This report describes the results of a series of 11 experimental flights which measured the characteristics of air-to-ground digital transmission in the VHF aeronautical mobile frequency band. The tests were conducted for the Federal Aviation Administration at National Aviation Facilities Experimental Center in Atlantic City, NJ. Digital transmission rates of 2400 and 4800 bps were used with minimum-shift-keying (MSK) as the baseband modulation format. The MSK signal was transmitted on a test frequency of 120.85 MHz using conventional, air/ground voice communication equipment.

A number of parameters were measured during the flights and an extensive description is given of the bit error rates which were encountered. Received signal level was also monitored, and data describing average signal level and signal fading are presented. Other parameters measured were clock slips, carrier losses, distribution of errors, and signal fading caused by aircraft maneuvering. The tests show that digital transmission rates of 2400 and 4800 bps can be supported, with existing FAA and ARINC equipment, at an average bit error rate near 5×10^{-5}.

17. Key Words	18. Distribution Statement
Aircraft, Communication, Digital Transmission, Minimum-Shift-Keying, Propagation.	Document is available to the public through the National Technical Information Service, Springfield, Virginia 22161

19. Security Classif. (of this report)	20. Security Classif. (of this page)	21. No. of Pages	22. Price
UNCLASSIFEID	UNCLASSIFIED	77	

PREFACE

This report was prepared for the U. S. Department of Transportation, Transportation Systems Center, under reimbursable order RA 76-2 411-0021. Certain commercial equipment, instruments, or materials are identified in this paper to adequately specify the experimental procedure. In no case does such identification imply recommendation or endorsement by the Office of Telecommunications, nor does it imply that the material or equipment identified is necessarily the best available for the purpose.

The authors would like to acknowledge the contributions of the NAFEC personnel. They are particularly indebted to Messrs. A. Swezeny, R. Erikson and J. Bernstein for their efforts in setting up and conducting the test flight. They would also like to acknowledge the contributions of Mr. D. Collins and Mr. R. G. FitzGerrell for their many helpful suggestions.
The authors are with the Institute for Telecommunication Sciences, Office of Telecommunications, U. S. Department of Commerce, Boulder, Colorado.

TABLE OF CONTENTS

LIST OF FIGURES

LIST OF FIGURES (Cont.)

LIST OF FIGURES (Cont.)

LIST OF TABLES

1. INTRODUCTION

The Federal Aviation Administration is currently investigating the feasibility of establishing a digital communication link between aircraft and the ground based air traffic control (ATC) system. This link is expected to be a more efficient transmission system since many of the routine voice messages can be transmitted more efficiently in a digital format with a corresponding reduction in work load on the air traffic controller and voice communication system. Other uses also can be envisioned for the facility that are not currently available in the present ATC system. For example, aircraft position, as seen by ground based radars, can be relayed to the aircraft from the ground stations. Another use might be to relay aircraft position, obtained by triangulation at the aircraft, to ground based computers in order to provide a more accurate determination of aircraft location. Some type of link also would be necessary in order to transmit maneuver commands in a ground based collision avoidance system.

A number of frequency bands have been considered for digital data transmission. The lowest frequency proposed to date is a VHF system operating in the existing 118-136 MHz aeronautical radio band. This system is the subject of investigation in the present report. Other frequencies that have been considered are the 1030 to 1090 MHz band currently used by the discrete address beacon system (DABS), and a new system at 1600 MHz. A satellite data link at 1600 MHz is also a possibility that would serve transoceanic as well as continental needs. Several other systems have the potential for transmitting data to serve special functions. The microwave landing system (MLS) and the differential OMEGA navigation system fall into this category.

This report describes a series of flight tests to observe the characteristics and problems of digital transmission at 118-136 MHz. All flight tests were conducted by Federal Aviation Administration personnel at the National Aviation Facilities Experimental Center (NAFEC) in Atlantic City, New Jersey. Equipment used during the test flights was assembled by Department of Commerce, Office of Telecommunications personnel, who also performed the final analysis of the data as described in this report.

The VHF digital transmission experiment, as configured in these tests, largely uses existing air/ground communication equipment. The airborne and ground transmitters and receivers are conventional double sideband, amplitude

modulated (DSB-AM) equipment that are normally used for voice communications on channels with either 25 kHz or 50 kHz nominal bandwidth. Digital modulation with minimum-shift-keying (MSK) as specified by the Federal Aviation Administration, is used with bit transmission rates of 2400 and 4800 bps.

2. DESCRIPTION OF FLIGHT TESTS

A pictorial diagram of a typical flight is shown in figure 1. As can be seen, information is recorded at the aircraft, a remote ground site, and at a tracking radar. All information is recorded on digital recorders along with a standard time reference so that the tapes subsequently can be integrated into one common tape for further analysis. The NAFEC extended area instrumentation radar (EAIR) continuously tracks the test aircraft and provides a record of the aircraft's azimuth elevation angle and slant range. The digital data link continuously transmits a test signal from the bottom antenna of a Gulf Stream aircraft at a frequency of 120.85 MHz. Aircraft parameters such as heading, roll, pitch, and yaw are recorded so that estimates of the aircraft's locations can be made during periods of poor radar coverage and also for correlation with test data. The data link receiving equipment is located approximately 1/2 mile from the end of NAFEC runway 13-31.* Records of bit and block errors, received signal level, and model status are made at this site.

A detailed block diagram of the equipment at the ground site is shown in figure 2. Basically, three receivers are used. Two of these are tuned to the data link signal while the third is tuned to a clear channel at 121.5 MHz to monitor local noise. The AN/GRR-23 has a bandwidth of 36 kHz (at -6dB level) and is the receiver that supplies the data link signal to the MSK demodulator. Receiver AGC is recorded as a measure of the input signal level. The TMR-5 receiver is also tuned to the data link signal and has a nominal bandwidth of 30 kHz. The primary difference between these receivers is that the TMR-5 is operated with the "squelch" disabled and a fast AGC response in order to provide a more detailed look at the fading structure of the received signal. Its AGC is sampled at a higher rate to enable reconstruction of fast fades.

---

* 1 mile = 1.609 kilometers

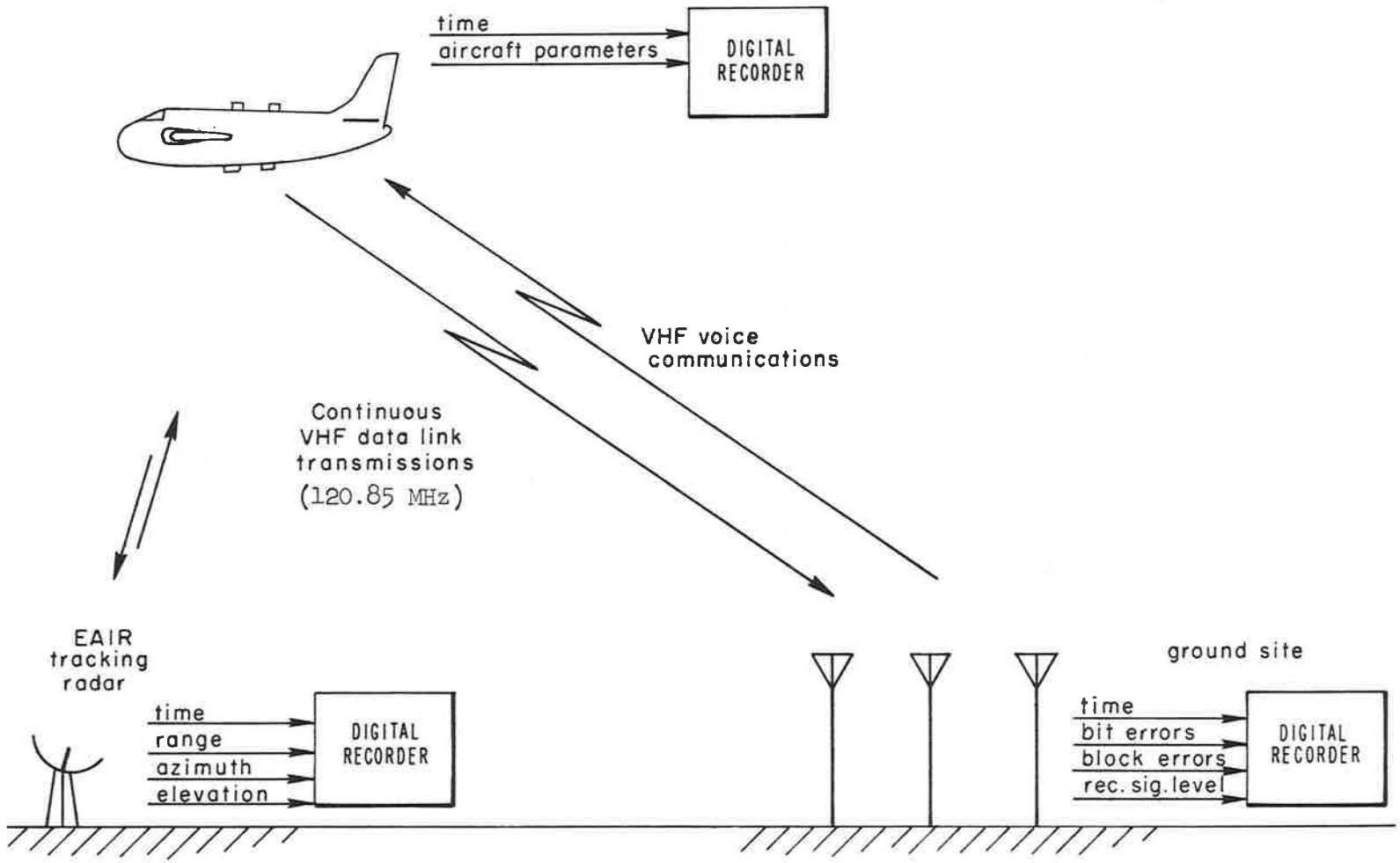

Figure 1. General description of tests.

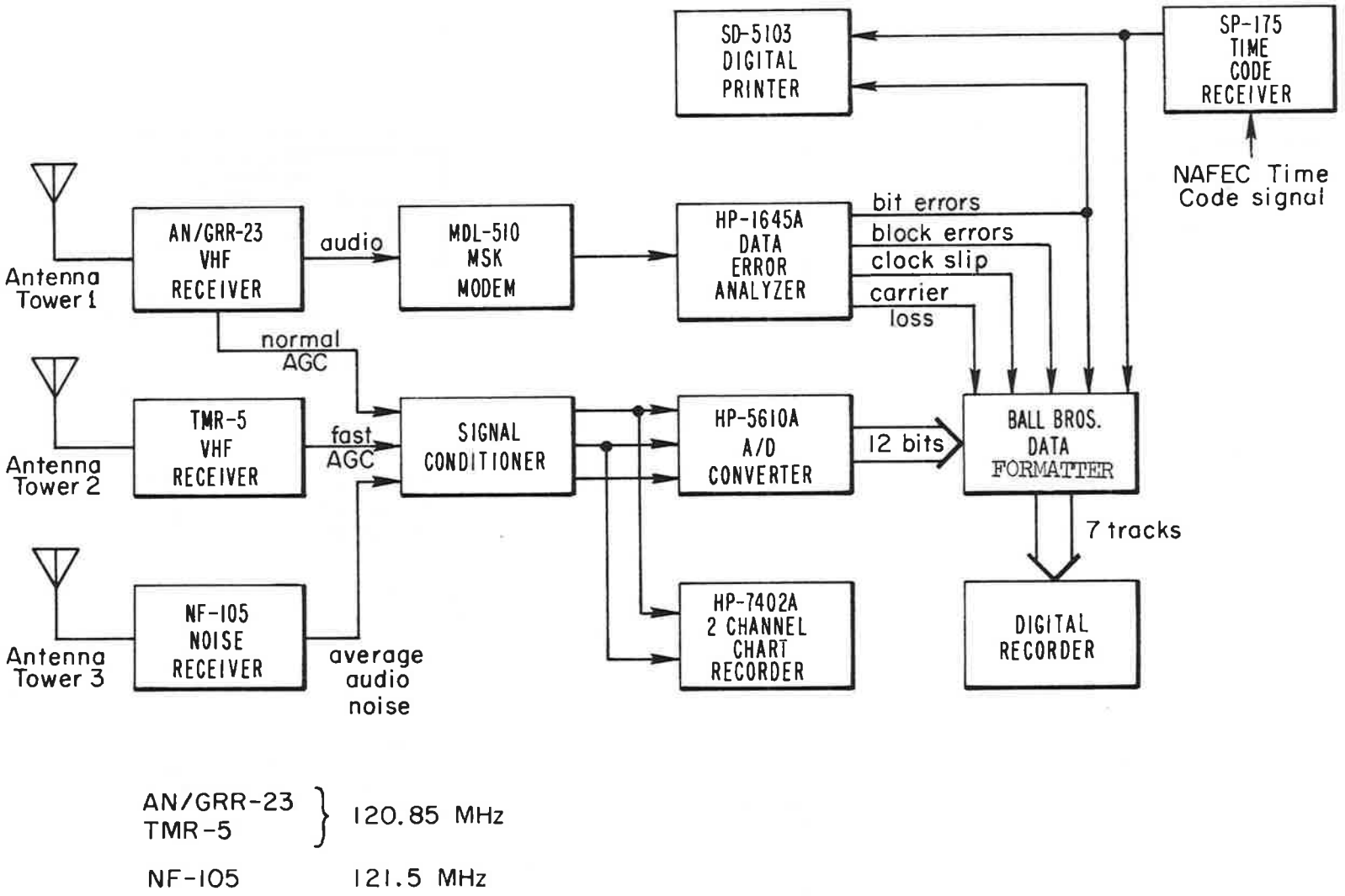

Figure 2. Block diagram of ground site equipment.

An NF105 noise receiver is used to monitor noise at the ground site. The receiver has a nominal bandwidth of 110 kHz and is tuned to a clear channel frequency of 121.5 MHz that normally is used only during emergency communications. Although this frequency is 650 kHz offset from the data link frequency, it is felt that the receiver provides a useful function in monitoring locally generated noise such as ignition noise or switching transients.

The AGC voltages from all three receivers are sent to separate DC amplifiers which appropriately prepare the signals for digitizing by the HP-5610A analog to digital converter/multiplexer. The output from the AN/GRR-23 VHF receiver also is sent to the MDL-510 MSK demodulator where it is demodulated into the received digital sequence that is subsequently analyzed for errors by the HP-1645A data analyzer. The HP-1645A used in these tests was modified to provide a continuous parallel output of bit errors, block errors, clock slips and carrier loss. Bit errors are measured in the data test set by comparing the received sequence with a stored replica of the transmitted pseudo random sequence. Error information from the data analyzer and outputs from the A/D converter are recorded on magnetic tape along with a time code. Analog records are also made during each flight by recording the AN/GRR-23 and TMR-5 AGC signals on a chart recorder. Bit errors and a 1 second time code are recorded on a digital printer.

A block diagram of the equipment in the aircraft is shown in figure 3. The digital sequence originates at the 1200 data analyzer where it is then sent to the MSK modem. The audio signal from the MSK modulator is connected to the AM input terminal of a conventional VHF transceiver and is transmitted via double side band amplitude modulation at a frequency of 120.85 MHz. A time code signal and the aircraft parameters are recorded simultaneously at the aircraft for subsequent merging with the ground site data. Voice communication between ground and aircraft is also available during the experiments.

A list of the parameters that are recorded at each of the sites is given in table 1. The sampling rate is 10 samples per second on all ground and EAIR radar signals, except for the TMR-5 receiver which is sampled at 400 times per second. All aircraft parameters are sampled at one sample per second.

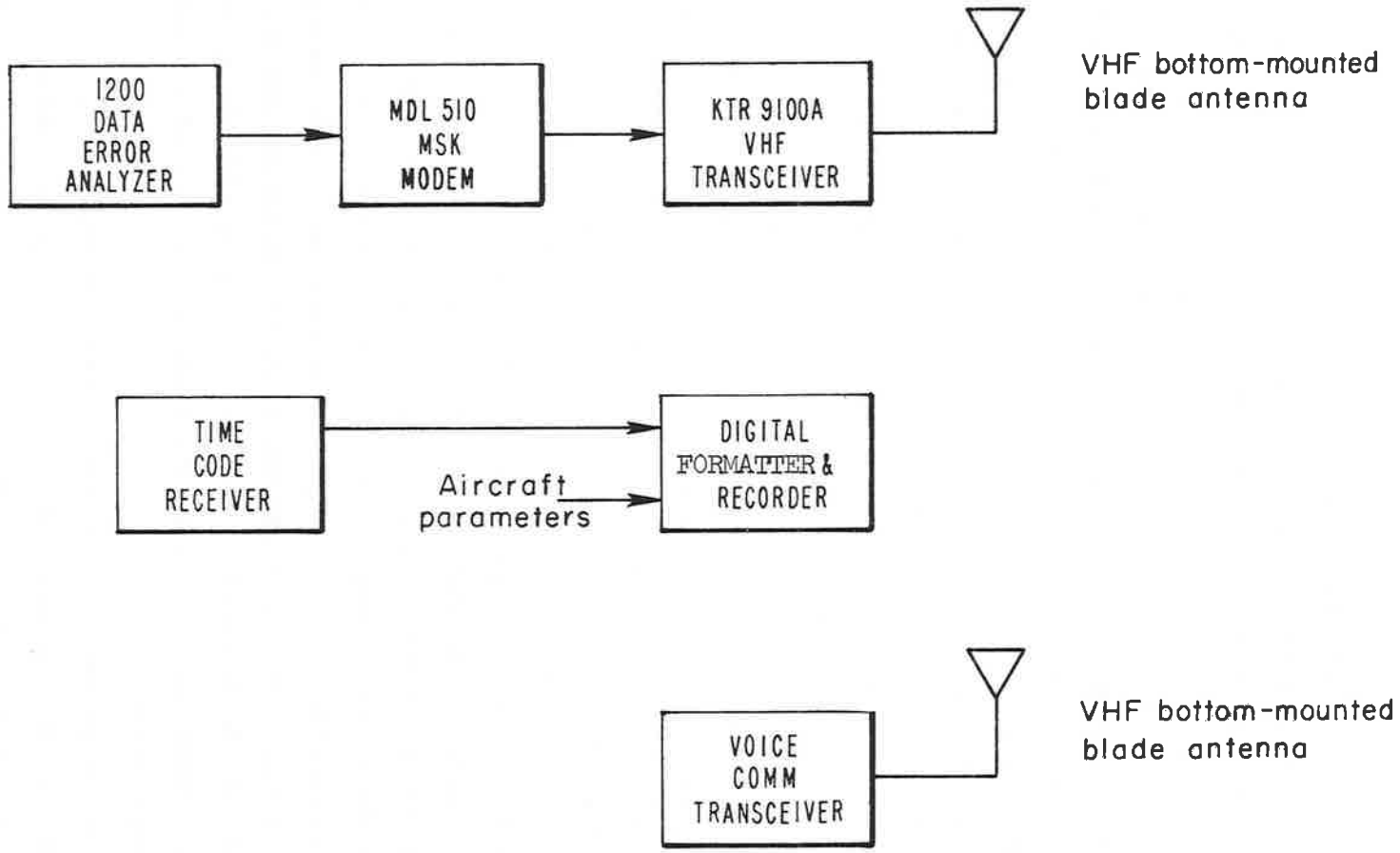

Figure 3. Block diagram of aircraft equipment.

Table 1. List of Parameters Recorded During the Flight Tests.

Ground Station
Bit Error Count
Block Error Count
Carrier Loss Count
Clock Slip Count
Time (day, hour, minute, second, tenth second)
Flight Number
Modem Status
Receiver Signal Level - AN/GRR-23
Receiver Signal Level - TMR-5
Receiver Noise Level - NF-105
Aircraft
Time (day, hour, minute, second, tenth second)
Heading
Altitude
Roll
Pitch
Yaw
Calibrate/Test Status
Flight Number
Modem
Radar
Slant Range
Azimuth
Elevation Angle
Time (day, hour, minute, second, tenth second)
Flight Number
Loss of Track
Beacon or Skin Track

Three CA-1781 VHF antennas (swastikas) are used at the ground site, each mounted on separate towers approximately 60 feet in height and 80 feet in separation.* These antennas are approximately omni-directional in the horizontal plane with a circular polarization. The aircraft antennas are conventional vertically polarized blade antennas mounted on the bottom of the aircraft.

* 1 foot = 0.3045 meters

3. MSK DATA TRANSMISSION

Digital information is transmitted during the flights with minimum-shift-keying (MSK) modulation. This section of the report describes some of the general characteristics of this type of modulation. Basically, MSK is a bandwidth conservation technique that potentially can transmit a binary sequence of rate R via a signal with a 3 dB bandwidth of approximately R/2. The MSK system as configured in these tests, however, requires an RF 3 dB bandwidth four times this value or 2R (Juroshek, 1973a, 1973b).

Assume for the moment that the digital transmission rate is 2400 bits per second (bps). With MSK, a binary "1" is transmitted by sending either a full cycle of a 2400 Hz tone, or a half cycle of a 1200 Hz tone as shown in figure 4. Similarly, the binary "0" is sent either with a full cycle of a 2400 Hz tone or a half cycle of a 1200 Hz tone. The choice of whether to use full or half cycles is dictated by the requirement that the transition between succeeding bits be phase continuous (this means that the time waveform has a continuous derivative). Thus, a sequence of digits is transmitted by a continuous series of full and half cycles of 1200 and 2400 Hz tones as shown in the lower half of figure 4. Note that a binary "1" always has a transition in the positive direction at the end of a bit period while the transition for a binary "0" is in the negative direction. The 4800 bps system has a similar diagram except that 2400 and 4800 Hz tones are used.

The MSK as depicted above commonly is referred to as a baseband signal in that it is generated at audio frequencies. The power spectral density of the baseband MSK signal is shown in figure 5 (Bennett and Rice, 1963). Probability of a bit error for the baseband MSK system in Gaussian noise with optimum detection is given by

$$P_e = \frac{1}{2}\left\{1\text{-erf } [E/N_o]^{1/2}\right\}, \qquad (1)$$

where E is the energy per bit and N_o is the noise power density as measured at the input to the demodulator. This expression is identical to the performance of bi-phase, coherent phase-shift-keying.

So far, we have considered only the baseband MSK signal. As noted, some additional circuitry must be used in order to translate the signal to the appropriate VHF frequency. Currently, the Federal Aviation Administration

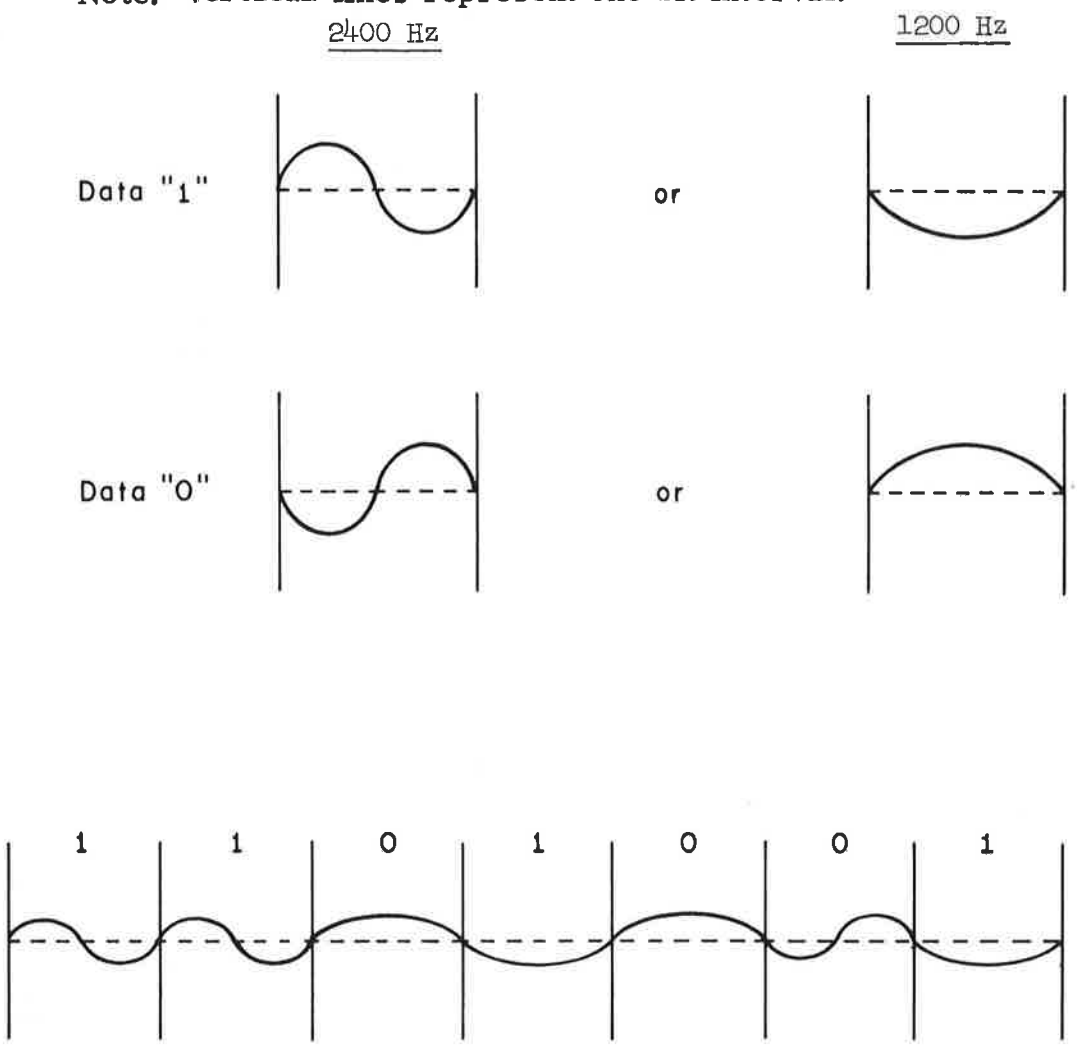

Bit values are determined by the slope at the end of a bit interval. Tones are selected to insure phase continuous keying.

Figure 4. Description of an MSK signal.

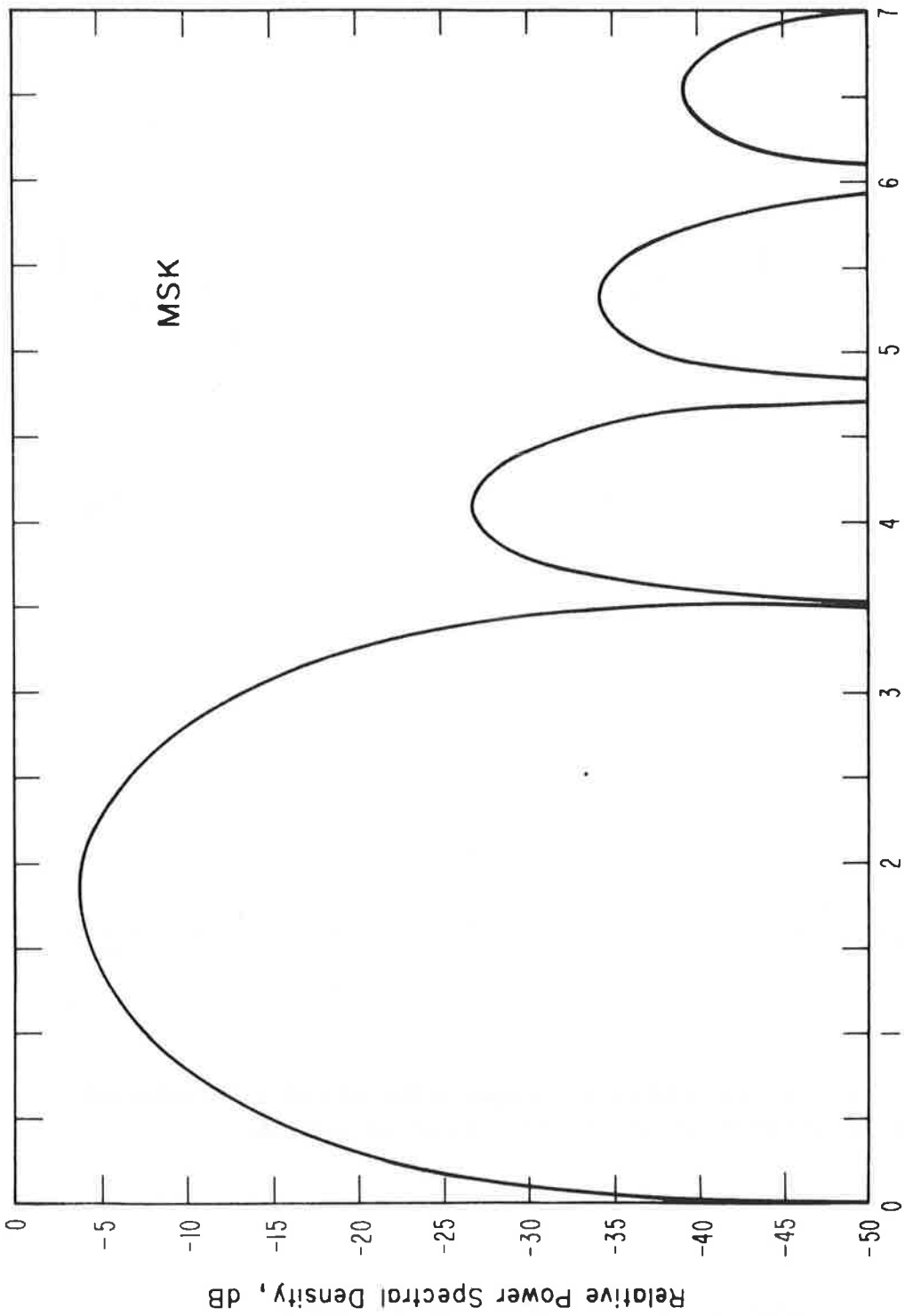

Figure 5. Power spectral density of a phase continuous, 2400 bit-per-second, MSK signal. Transmit tones are 1200 and 2400 Hz.

is using conventional double sideband amplitude modulation to transmit the signal. The MSK baseband signal is simply connected to the audio input terminal of a conventional air/ground VHF transmitter and the percentage of modulation is set at 85%.

Generally, this type of transmission is compatible with existing air/ground voice communication equipment. One exception is that some units require modification to avoid distortion due to nonlinear phase response in the audio circuitry, and to increase AGC attack times. The equipment used in these tests is able to pass audio signals from 400 Hz to 9.6 kHz within ±6 dB of the 1000 Hz level. The only unit modified was the AN/GRR-23.

Various schemes have been proposed for synchronization of MSK. One of these is the transmission of an initial sequence of "1's" and various ASCII data characters to allow for receiver stabilization, establish bit sync, and resolve a potential phase ambiguity due to the modulation. The modems in these tests ran continuously, transmitting the pseudo-random sequence of bits that originated in the HP-1645A data test set. No special synchronizing sequence was used at any time during the tests. After a signal dropout, the demodulator simply relies on the pseudo-random sequence to re-establish bit synchronization. Block synchronization is not necessary since this is automatically done by the data test sets. Also, there is no need to resolve a positive or negative phase ambiguity since this is correctly resolved prior to the first flight and does not change during the tests.

4. TEST RESULTS

This section describes the results of 11 flights that were conducted at NAFEC and a general summary for each flight is given in table 2. As can be seen, the flights are numbered from 5 through 16 with flight number 8 omitted. The flights are generally towards one of three directions: New York City; Scranton, Pennsylvania; or Norfolk, Virginia. A map showing the approximate path of each flight is presented in figure 6. The New York City flights can be classified best as "over water" while the Scranton flights are "over land". The Norfolk flights can be considered a combination since the flight path traverses both land and water.

Table 2. General Summary of Flights

Flight No.	Date	Start Time (EST)	Direction	Max Distance (n mi)	Max Altitude (ft)	Flight Duration (hrs)	Bit Rate (bps)	Comments
5	12/6/74	06:02	New York	112	18,049	1.3	2400	Landed MacArthur Field
6	12/12/74	14:30	Scranton	136	20,904	1.2	2400	Landed Philadelphia Int.
7	12/19/74	06:18	Scranton	128	18,158	1.2	2400	
9	12/23/74	13:16	Norfolk	191	17,201	2.6	2400	To Sea Isle Radial
10	1/7/75	09:05	Norfolk	191	16,259	2.4	2400	
11	1/8/75	13:04	New York	112	17,633	1.4	2400	1 mile from MacArthur Field
12	2/11/75	13:25	Norfolk	187	17,015	2.4	4800	
13	2/13/75	09:09	Norfolk	185	16,907	2.1	4800	Landed Cape May
14	2/13/75	13:58	New York	115	16,028	1.5	2400	7500 feet approach to McArthur
15	2/21/75	13:45	Scranton	129	18,845	1.0	4800	
16	2/21/75	15:05	Scranton	132	18,110	1.1	4800	

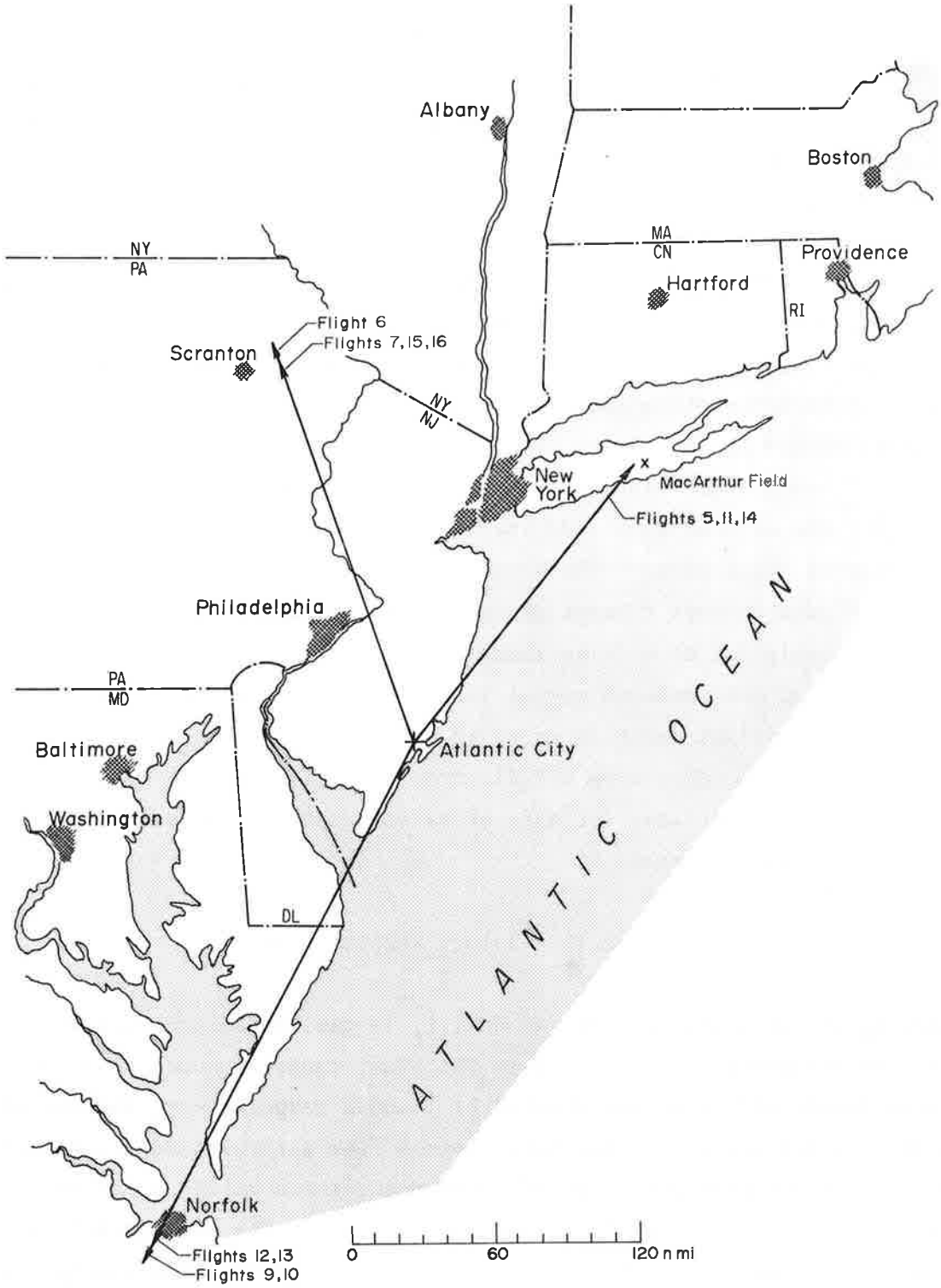

Figure 6. Map showing approximate flight paths.

4.1 Received Signal Level

The first test parameter to be examined is received signal level in microvolts versus aircraft slant range. Received signal in this section of the report refers to the average level of the data link signal reference to the antenna input terminal of the AN/GRR-23 receiver. The slant range is obtained from the recorded radar information with each measurement corrected by a computer to reflect distance relative to the ground site rather than the EAIR radar. Often during a flight, the radar lost track before the data link became inoperative. In order to obtain slant range during these periods, the flight path was reconstructed using "dead reckoning" based on heading altitude and airspeed information recorded in the aircraft. This process generally provides satisfactory results. Two examples of this process are shown in figures 7 and 8 where slant range versus time is plotted. The solid lines represent the data as supplied, where periods of no radar contact are simply connected by solid lines. The reconstructed flight paths are shown by dashed lines. Figure 7 shows a point where momentary radar contact was obtained, and is probably due to a false radar track.

A plot of the received signal level values, as averaged over a 10 sec period, versus slant range is shown in figure 9. This plot is a scatter diagram of points taken from all flights, and all altitudes between 0 and 20,000 ft. A theoretical estimate of received signal power, assuming free space transmission losses, is

$$P_R = P_T - 32.45 - 20\log f - 20\log(1.85d) - L + G \qquad (2)$$

where P_R is the received power in dBw, P_t is the transmitter power (14 dBw), f is the frequency in MHz, and d is the slant range in nautical miles. The system losses and gains are denoted by L and G respectively, and are also in dB. System losses are the total losses from aircraft and ground site cables, while system gains are the combined antenna gains (relative to isotropic) from the aircraft and ground antennas. The data presented later in the report will show that the losses and gains are approximately equal and therefore,

$$-L + G = 0 \qquad (3)$$

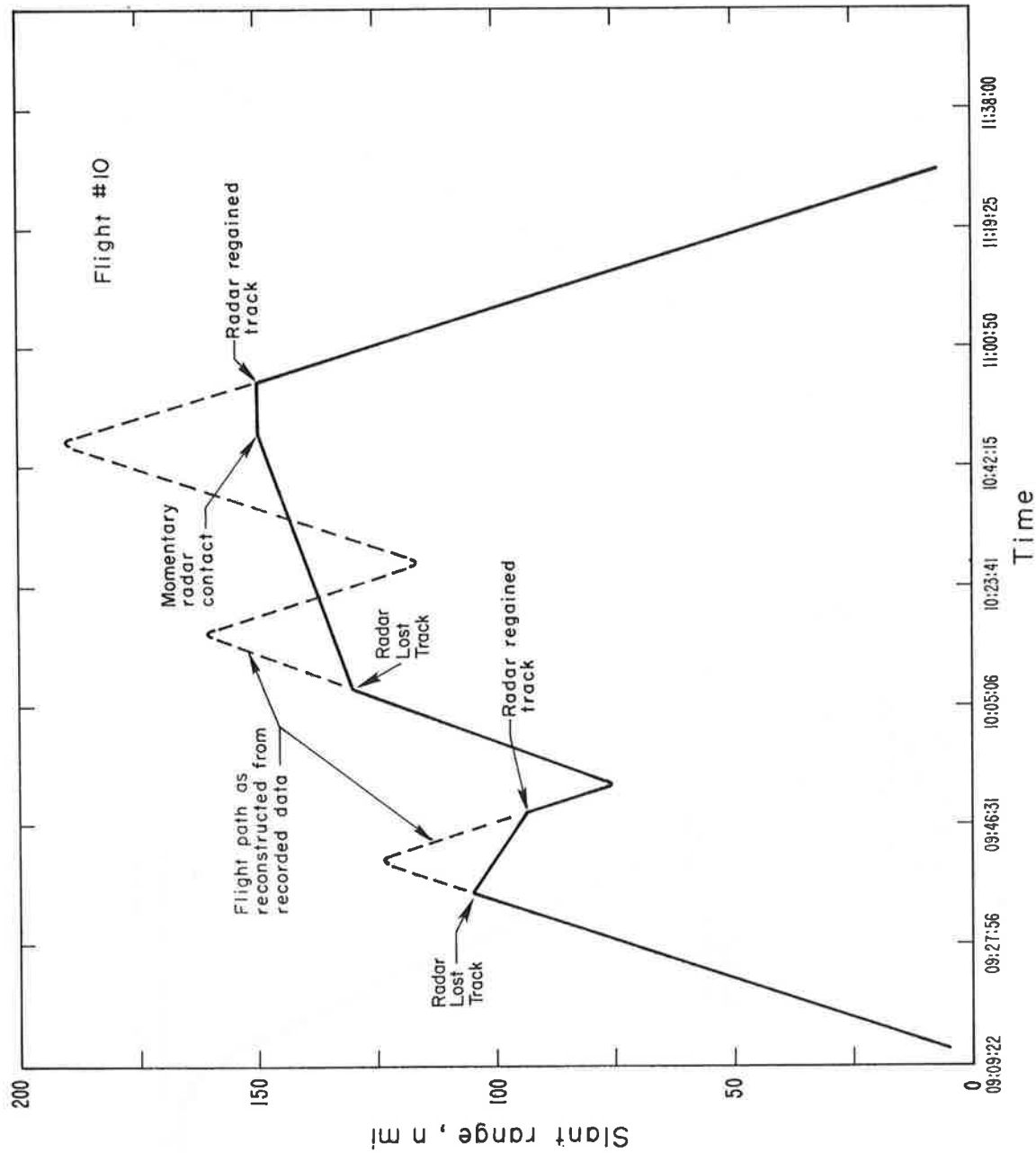

Figure 7. Plot of slant range versus time for flight 10.

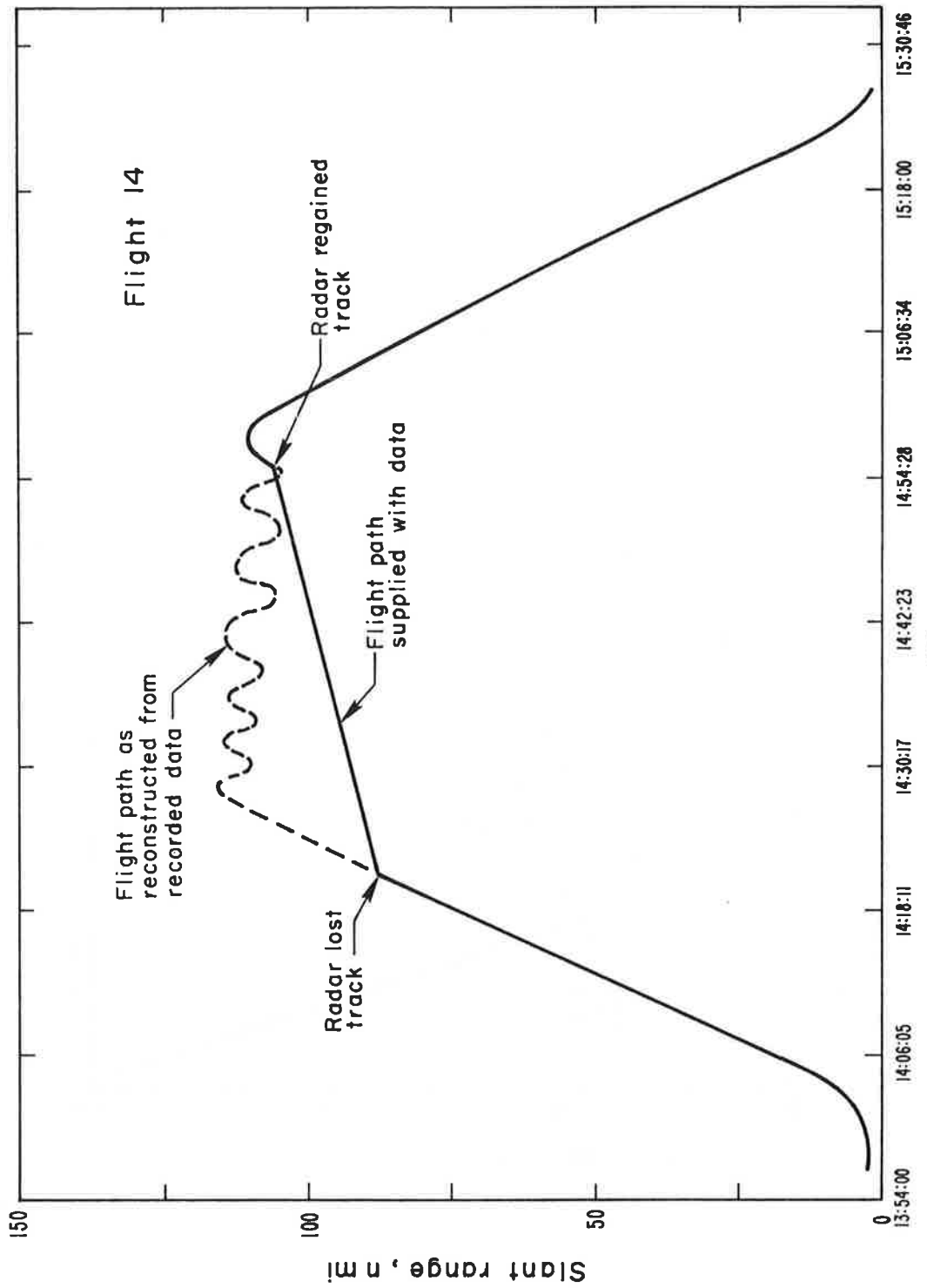

Figure 8. Plot of slant range versus time for flight 14.

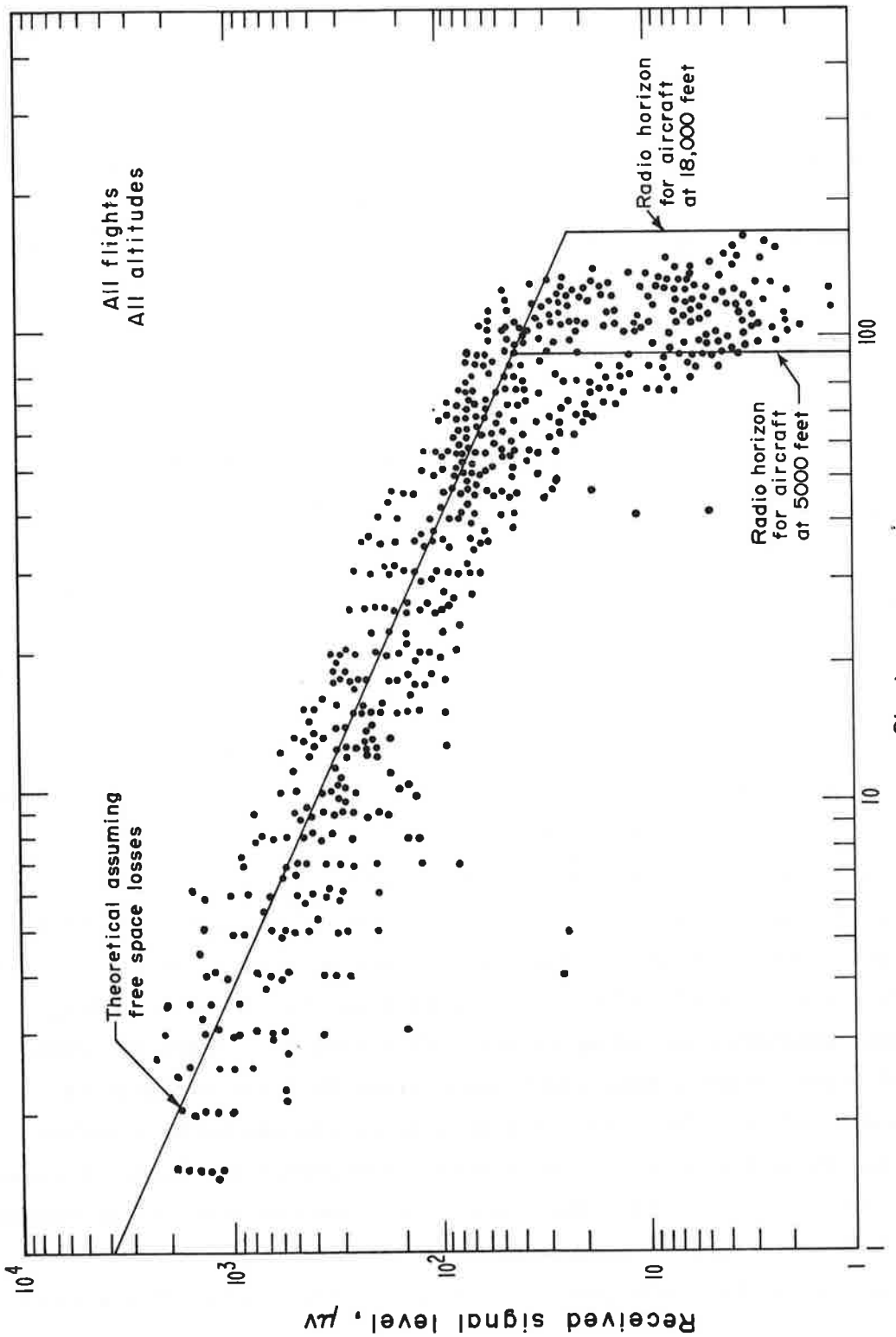

Figure 9. Average received signal level versus slant range for all aircraft altitudes.

which means that (2) can be expressed as

$$P_R = P_T - 32.45 - 20\log f - 20\log(1.85d). \tag{4}$$

For convenience we will include polarization mismatch losses in G and simply view polarization losses as a reduction in antenna gain. The solid line in figure 9 is a plot of equation 4. The signal level in volts is related to P_R by

$$V = (50 \times 10^{P_R/10})^{1/2}, \tag{5}$$

assuming a 50 ohm receiver input impedance. Figure 9 shows that the signal level rapidly decreases as the aircraft approaches the radio horizon. The radio horizons for an aircraft at 5,000 and 18,000 ft as shown in figure 9, are calculated using the approximation

$$d_h = 0.869(2h)^{1/2}, \tag{6}$$

where d_h is the distance to the radio horizon in nautical miles and h is the aircraft's altitude in feet above mean sea level. This approximation assumes an effective earth radius of 4/3 the true earth radius. The approximation also neglects the height of the ground site antenna. As can be seen, the experimental data generally agree with the theoretical calculation with the measured signal levels, on the average, equal to the theoretical calculation.

In order to isolate the effects of aircraft altitude, the preceding data are shown replotted according to aircraft altitude. Figure 10 shows the received signal level versus slant range given that the aircraft is between 0 and 6,000 ft. The only major difference appears to be a rather sharp decrease in signal level as the aircraft approaches the 6,000 ft radio horizon. Figure 11 is a similar plot except that now the aircraft is between 6,000 and 12,000 ft. Again, the only major difference is an extension of the radio horizon due to the higher aircraft altitude. A plot of the data

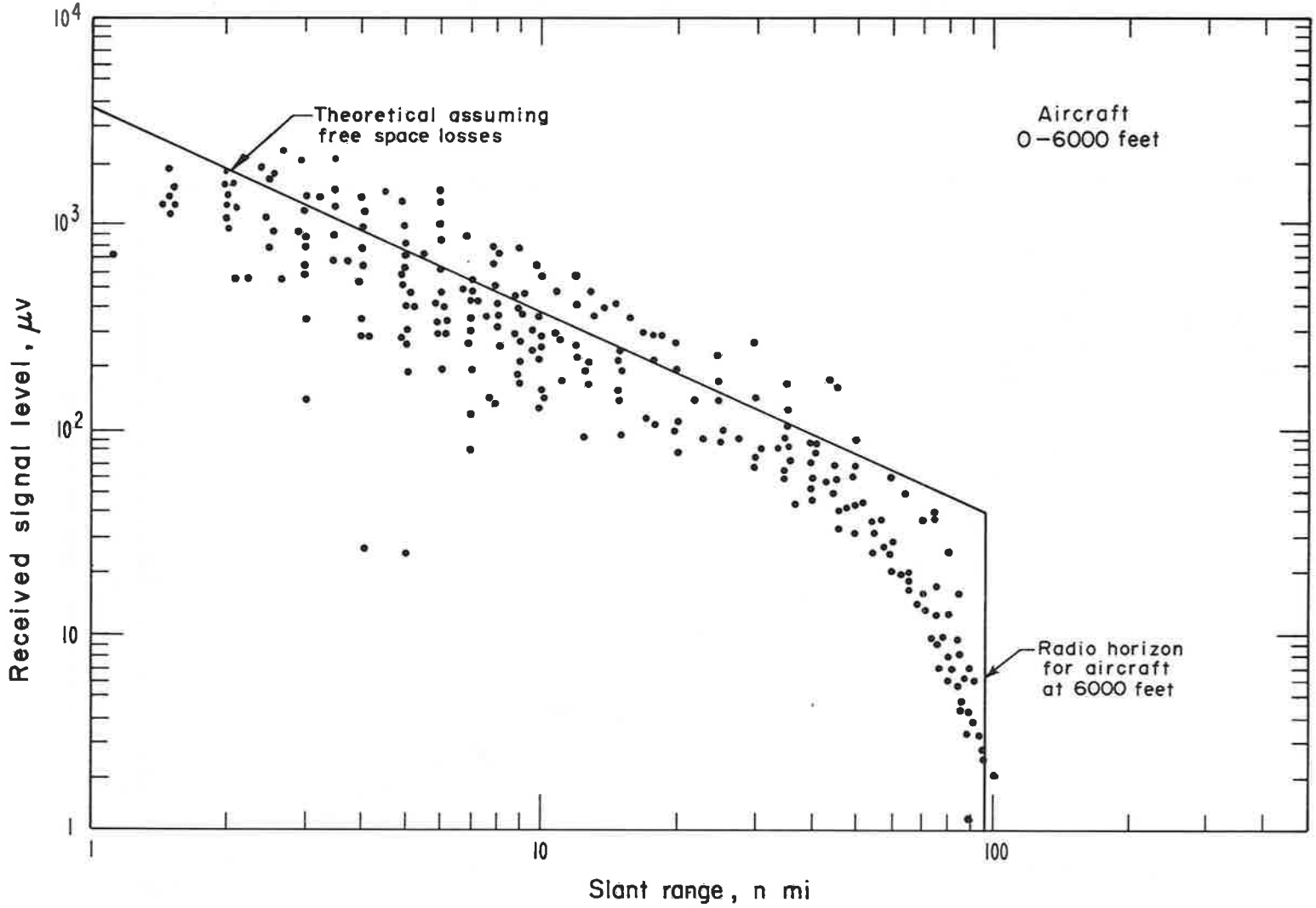

Figure 10. Average received signal level versus slant range given that the aircraft was between 0 and 6000 ft altitude.

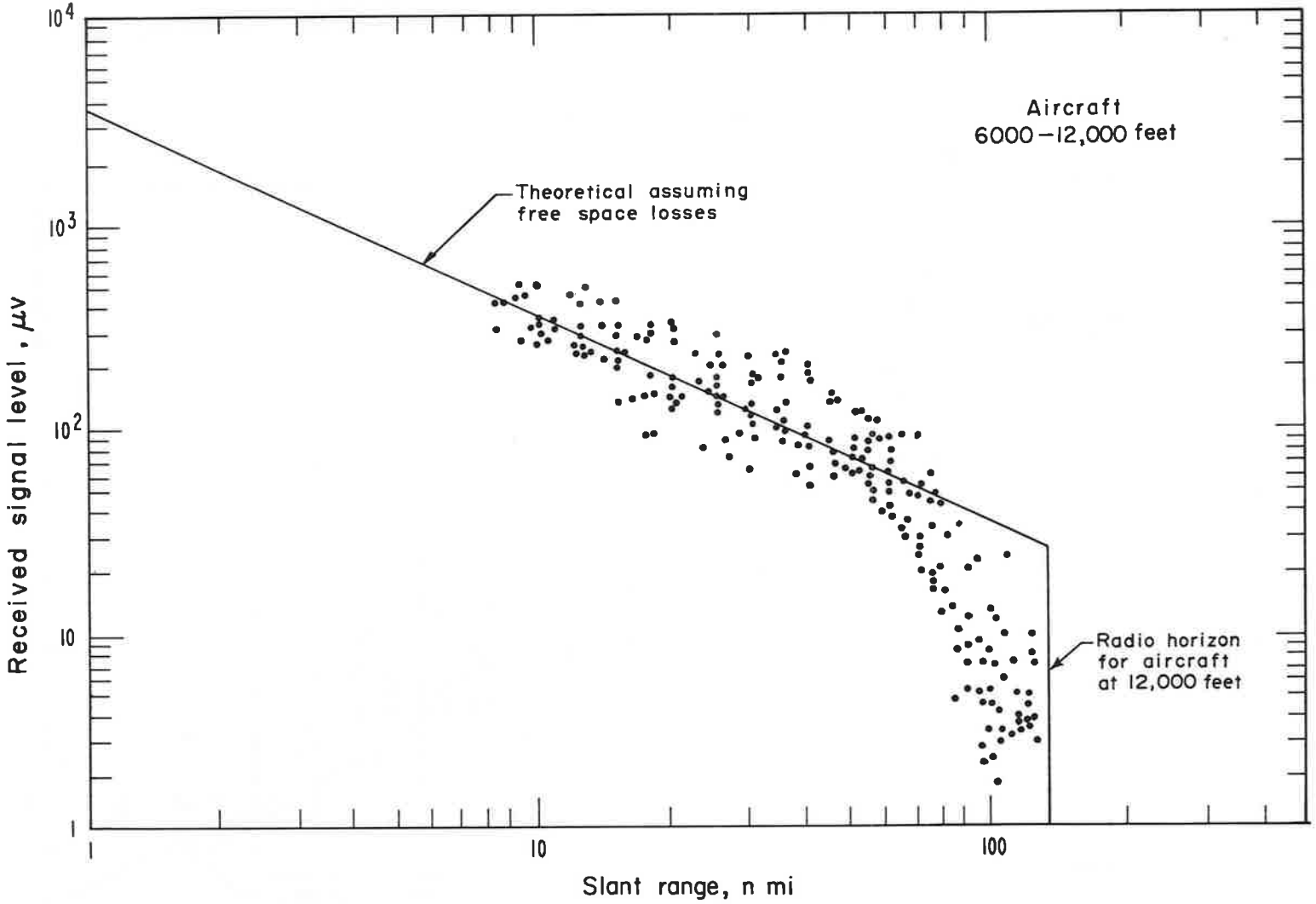

Figure 11. Average received signal level versus slant range given that the aircraft was between 6000 ft and 12,000 ft altitude.

when the aircraft is between 12,000 and 18,000 ft is given in figure 12. As with the other graphs, the only major difference appears to be the extension of the radio horizon due to the increased aircraft altitude. There are no data samples at slant ranges less than 20 n mi in figure 12, since the test aircraft did not fly at high altitudes when it was close to the NAFEC facility.

In summary, the average value of the signal level samples, as shown in figures 9 through 12, is reasonably well described by equation (4). The average of the samples is approximately equal to the theoretical calculation. Thus, the assumption of equal system gains and losses, in equation (3), appears to be a reasonably good assumption in these tests. This system has a loss L that is estimated to be 4 dB which is composed of 3 dB ground site cable losses, that were measured, and 1 dB aircraft cable losses. The aircraft cable losses were not measured because of accessibility problems. Thus, a reasonable estimate for G during these tests is 4 dB.

Occasionally signal level samples can be seen in the figures that are 6 dB above the theoretical calculation. This is probably due to the addition of the ground reflected signal and the direct signal which can, during favorable conditions, give a 6 dB increase in signal strength. The antennas can also contribute to this increase in that the antennas are likely to have gains that exceed the average in certain directions.

4.2 Signal Fading

So far, we have considered only the value of the received signal level as averaged over 10 seconds. Next, we will examine the variability in the signal during this interval. This variability is called signal fading and denotes the maximum change or peak-to-peak variation in signal level within the 10 seconds.

A graph showing fading as a function of slant range is given in figure 13. Note that relatively severe fading is encountered when the aircraft is from 1 to 10 n mi from the ground site, with a maximum value of 20 dB. When the aircraft is 10 to 20 n mi out, the fading is substantially less with the maximum now of only 8 dB. The magnitude of the fading continues to decrease with increasing slant range until, at 100 n mi, the maximum fading is only 2.5 dB. The increase in fading when the aircraft is in close is probably due to the combination of ground reflections with the direct

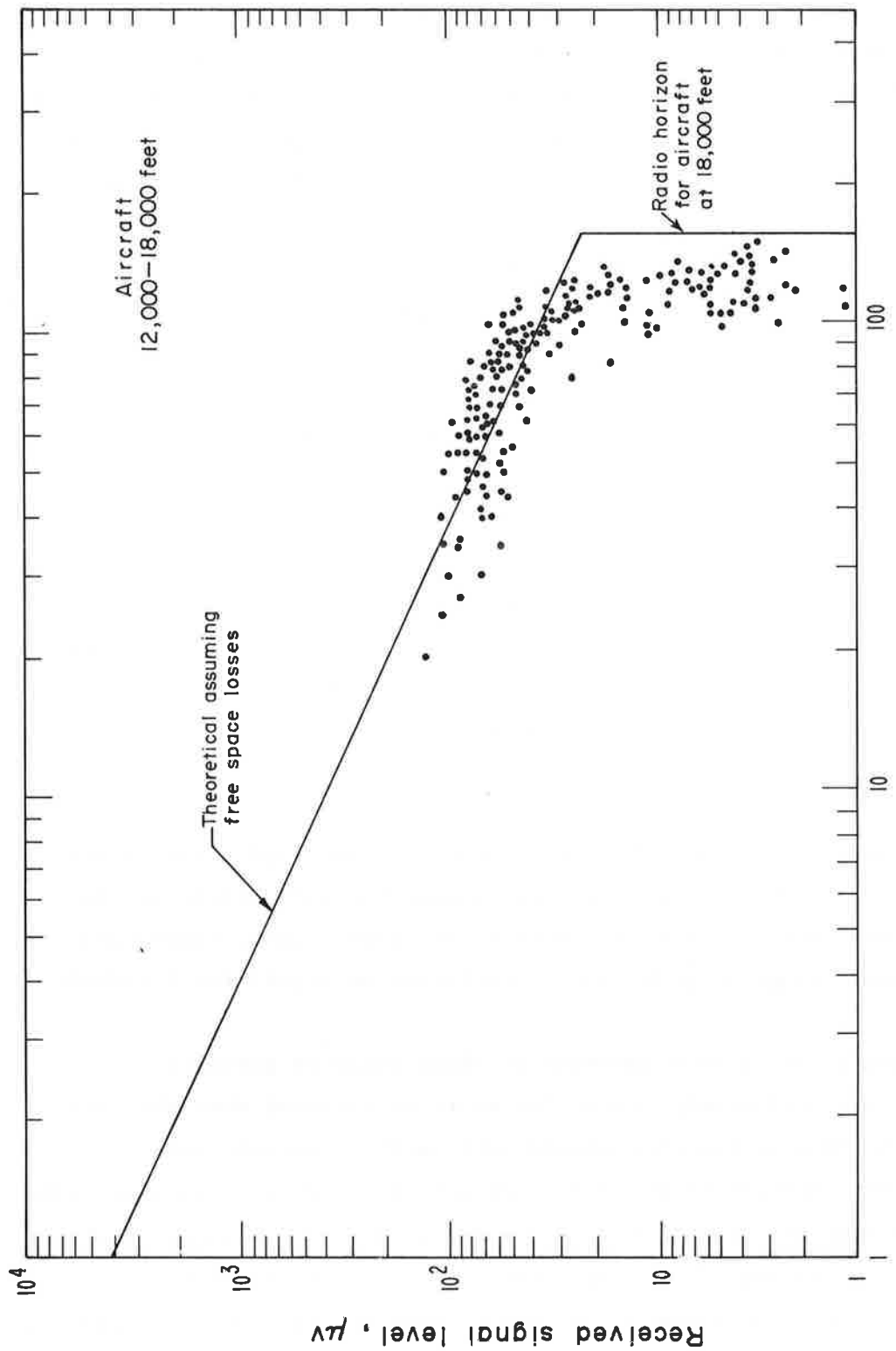

Figure 12. Average received signal level versus slant range given that the aircraft was between 12,000 and 18,000 ft altitude.

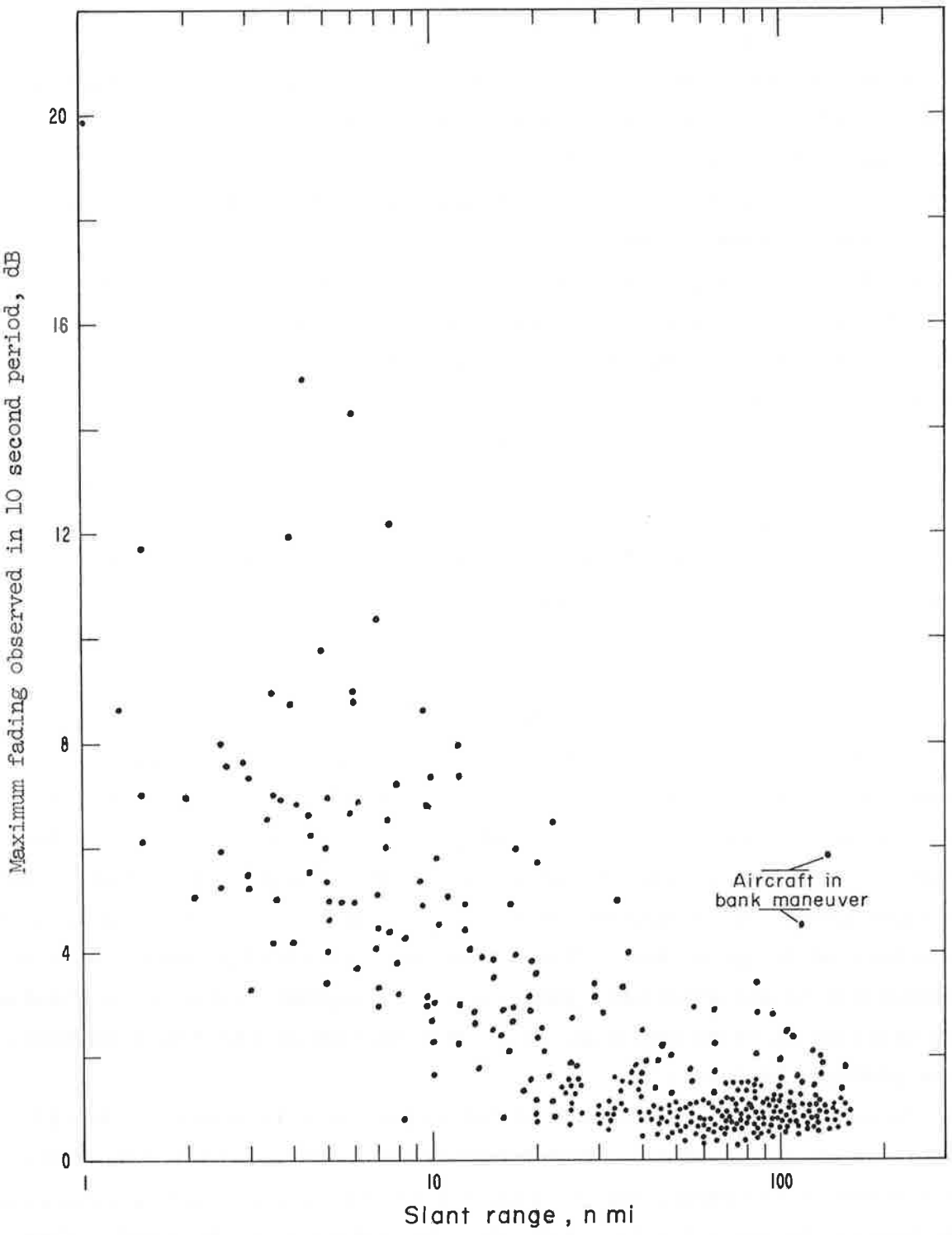

Figure 13. Peak-to-peak fading observed in a 10 second period as a function of slant range.

line-of-sight signal. When the aircraft is in close the angles between the directed and reflected rays can quickly change. However, when the aircraft is relatively far from the ground site, the geometry and angles involved remain constant and, therefore, signal changes are less likely.

Figure 14 is included in the report as a sample of the different types of fading structure that were encountered during the tests. These samples are obtained by sampling the AGC of the TMR-5 receiver at a rate of 400 samples per second. The upper trace in the figure shows the nearly constant conditions that are encountered at large slant ranges, while the lower two traces show the relatively severe fading that is encountered when the aircraft is near the receiving site.

Three samples similar to the lower two traces in figure 14 were analyzed by hand in order to estimate the rate at which the fading occurs. This analysis showed fading anywhere from a fraction of a cycle per second up to a maximum of 2 cycles per second. The reader is cautioned that this is a limited analysis and is included here only to give a rough idea of the fading rate.

4.3 Measured Bit Error Rate

The occurrence of bit errors during the tests is determined by a number of factors. Obviously, noise is something that is always present and a potential source of error. Inadequate filtering can also cause bit errors and is often a problem that is difficult to spot. Other factors that can cause errors are fading due to banking or improper synchronization as the radio horizon is approached. Also errors are occasionally noted that are attributable to uncontrollable problems like equipment failures, overheating, test switches in wrong position, etc. This section of the report examines these problems in detail.

An example of the occurrence of bit errors as a function of elapsed time is shown in figure 15. This figure essentially shows the bit errors per 1 second data sample, versus time, for flight number 5 and is typical of what happens during a flight. Note that the majority of the samples show either 1 or 2 bit errors per 1 second sample. Also, there are two periods when the transmitter is off due to equipment problems. Fortunately, the data test set is disabled automatically during these periods so that errors are not

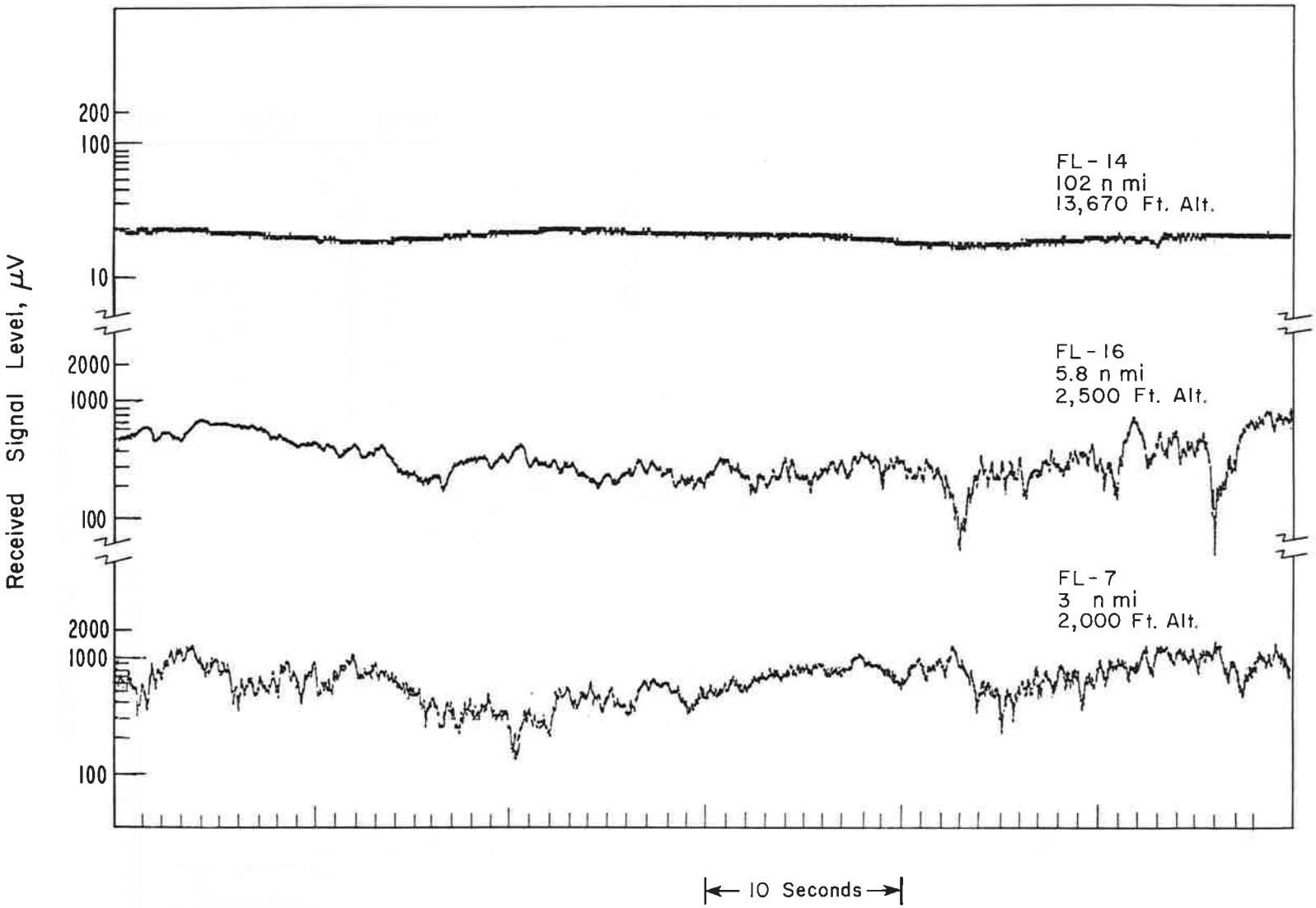

Figure 14. Example of different types of fading that were encountered during the tests. Flight number, aircraft slant range, and altitude are shown for each sample.

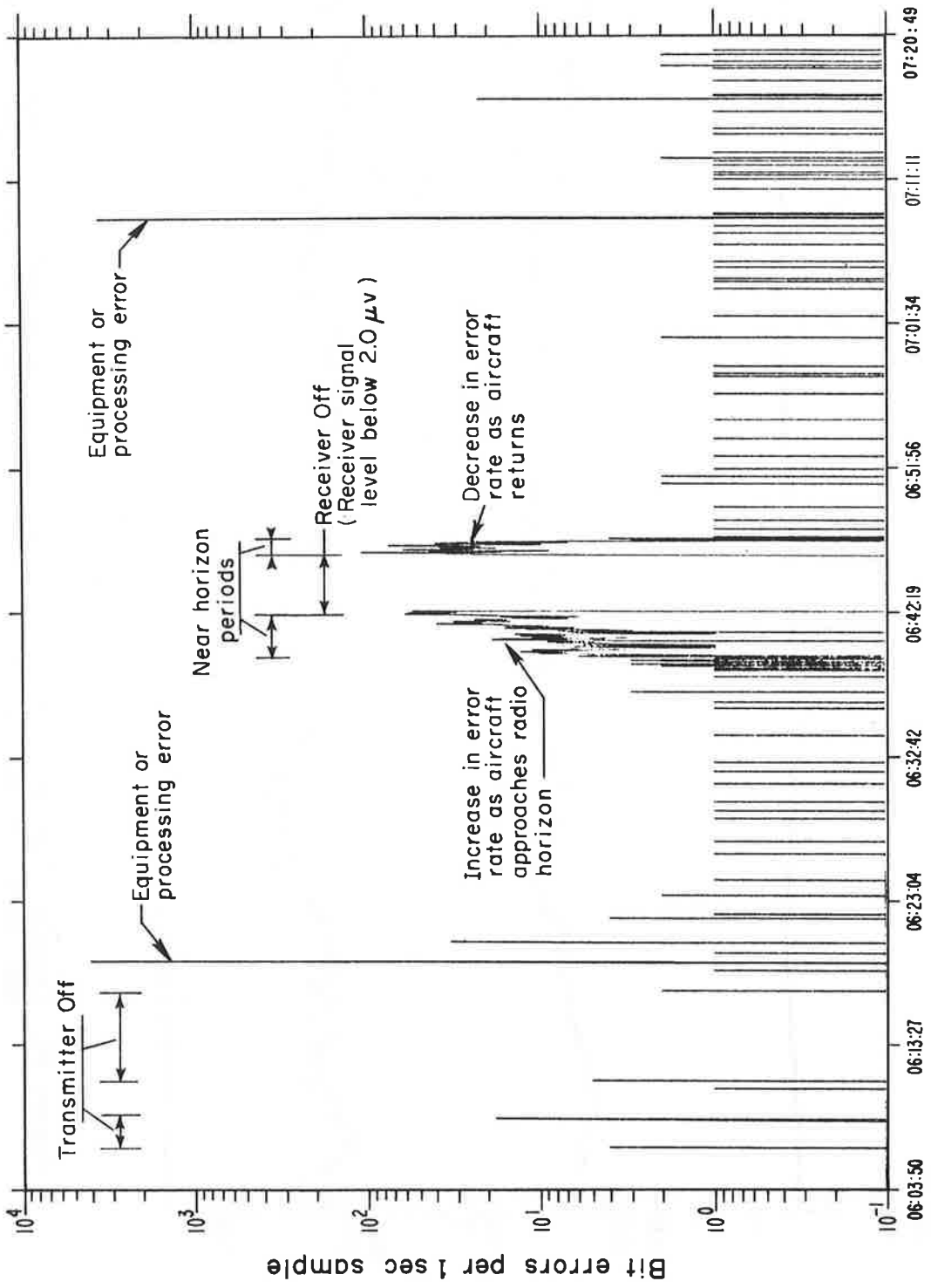

Figure 15. Bit errors per 1 second data sample versus time for flight 5.

accumulated. As the flight progresses, one can see occasional bursts of errors up to 20 or more bits.

As the aircraft approaches the radio horizon (at time 06:38), the error rate suddenly begins to increase. This increase continues until the signal reaches the 2 μV receiver squelch threshold. At this point, the data test set recognizes the loss of carrier and disables the error-counting circuitry. The return across the radio horizon is the reverse situation in that the receiver squelch is first enabled. The data test set then begins to recognize the presence of data and begins to count errors at a very high error rate. Eventually, a reasonably stable error rate condition is achieved. The high bit error rate period when the aircraft is near the radio horizon will be called the "near horizon period" throughout this report and will be analyzed in detail later in the report.

Two instances in figure 15, show a bit error count of 4096 within a 1 second sample. This, of course, is impossible since the bit rate of the system is only 2400 bps. Unfortunately, this problem was not discovered until after all the data had been taken. The problem appears to be an occasional erroneous count due to equipment problems. In any event, this erroneous count did not create a problem since the count is always 4096 or 2^{12} and, therefore, can easily be removed from the data.

The average bit error rate (P_e) for each flight using the "raw" data as received from NAFEC is shown in figure 16. This figure averages all errors including the 4096 counts. As can be seen, the results range anywhere from 4.1×10^{-2} to 1.6×10^{-5}. The shaded columns denote 4800 bps flights.

Figure 17 is similar except that now the errors due to "equipment and operational problems" are removed. All periods during which there are equipment failures, overheating, data switches in wrong positions, and the 4096 counts are removed during these calculations. The average bit error rate for some tests drops an order of magnitude while some tests remain the same since there are no equipment or operational problems on those flights.

Similar results also can be presented by removing those periods when the aircraft is in the near horizon regions. These results are shown in figure 18, where only the near horizon errors are removed. Therefore, equipment and operational errors are included. Figure 19 presents the other case where both equipment, operational, and near horizon errors are removed.

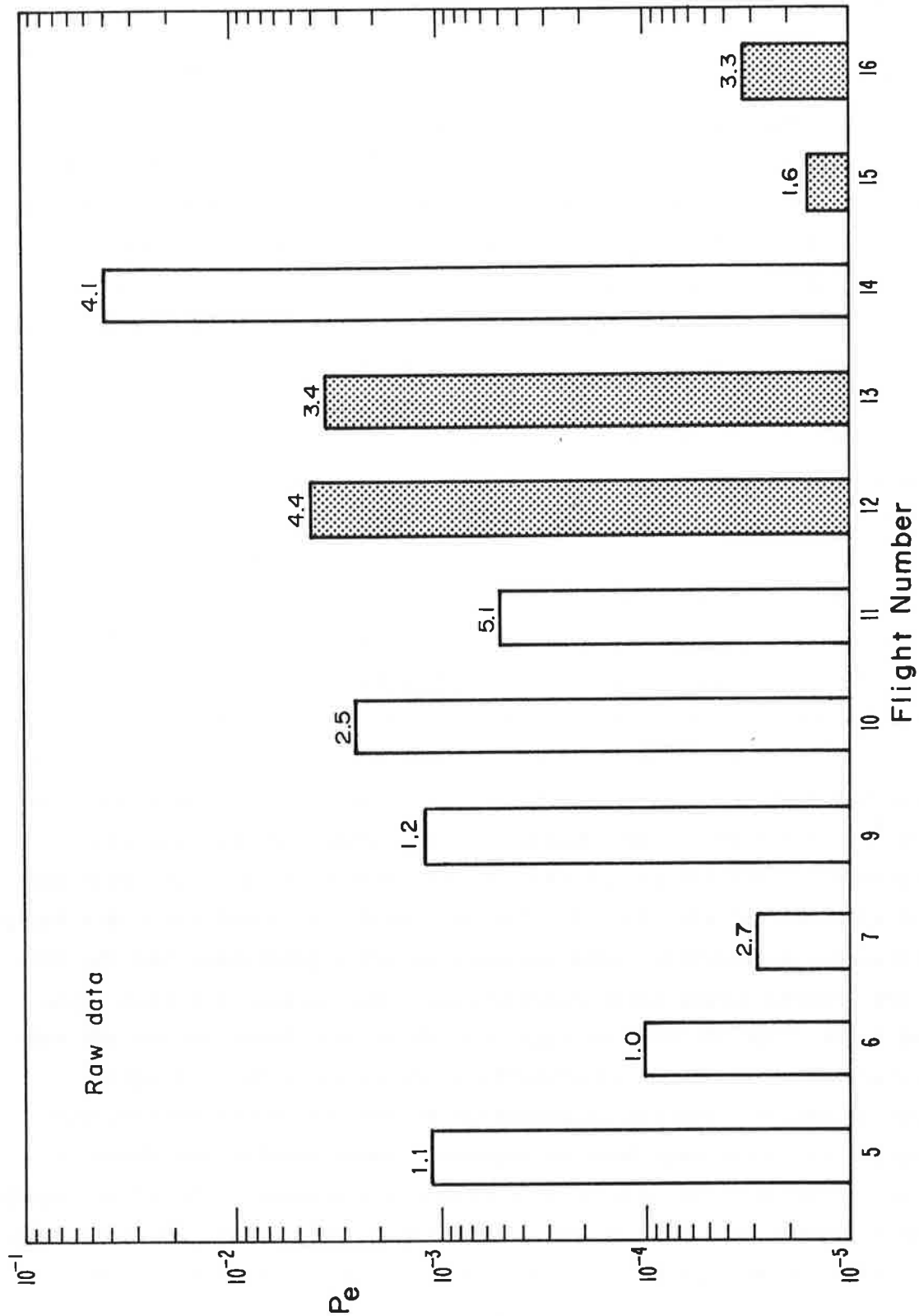

Figure 16. Average bit error rate for each flight using data supplied by NAFEC. Includes errors due to equipment and operational problems. Shaded areas denote 4800 bps flights.

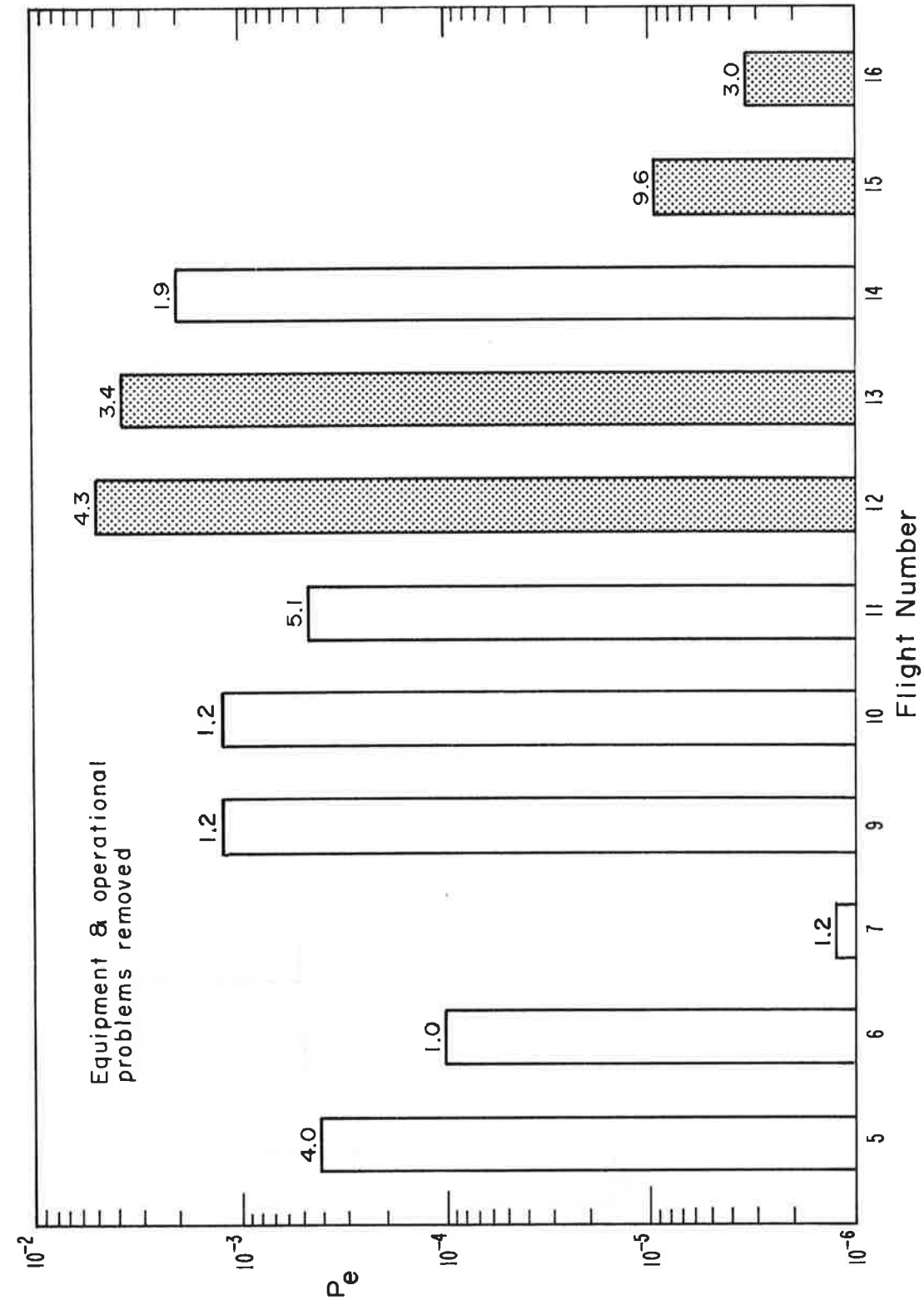

Figure 17. Average bit error rate for each flight removing equipment and operational problems.

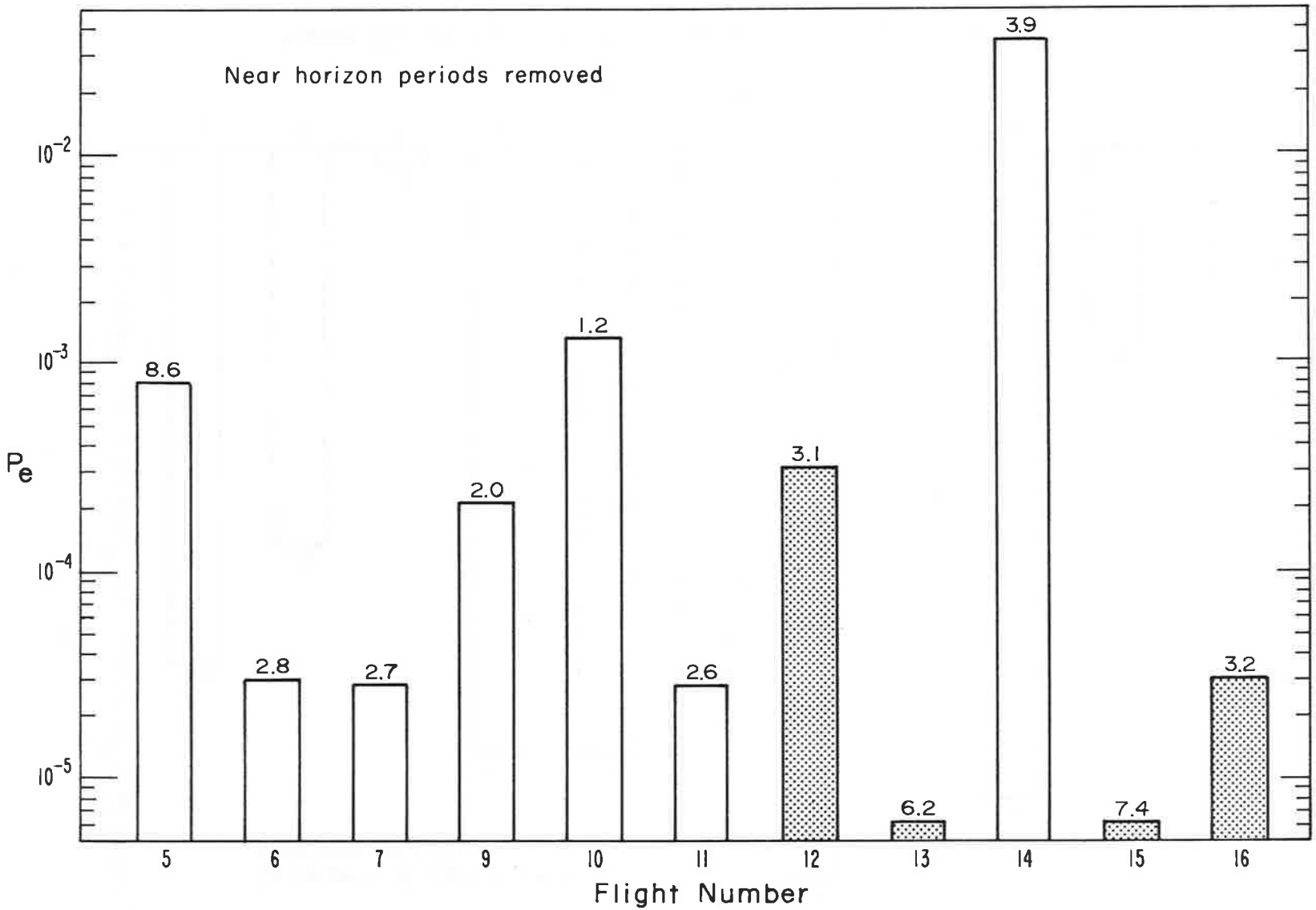

Figure 18. Average bit error rate for each flight removing the near horizon or high error rate periods.

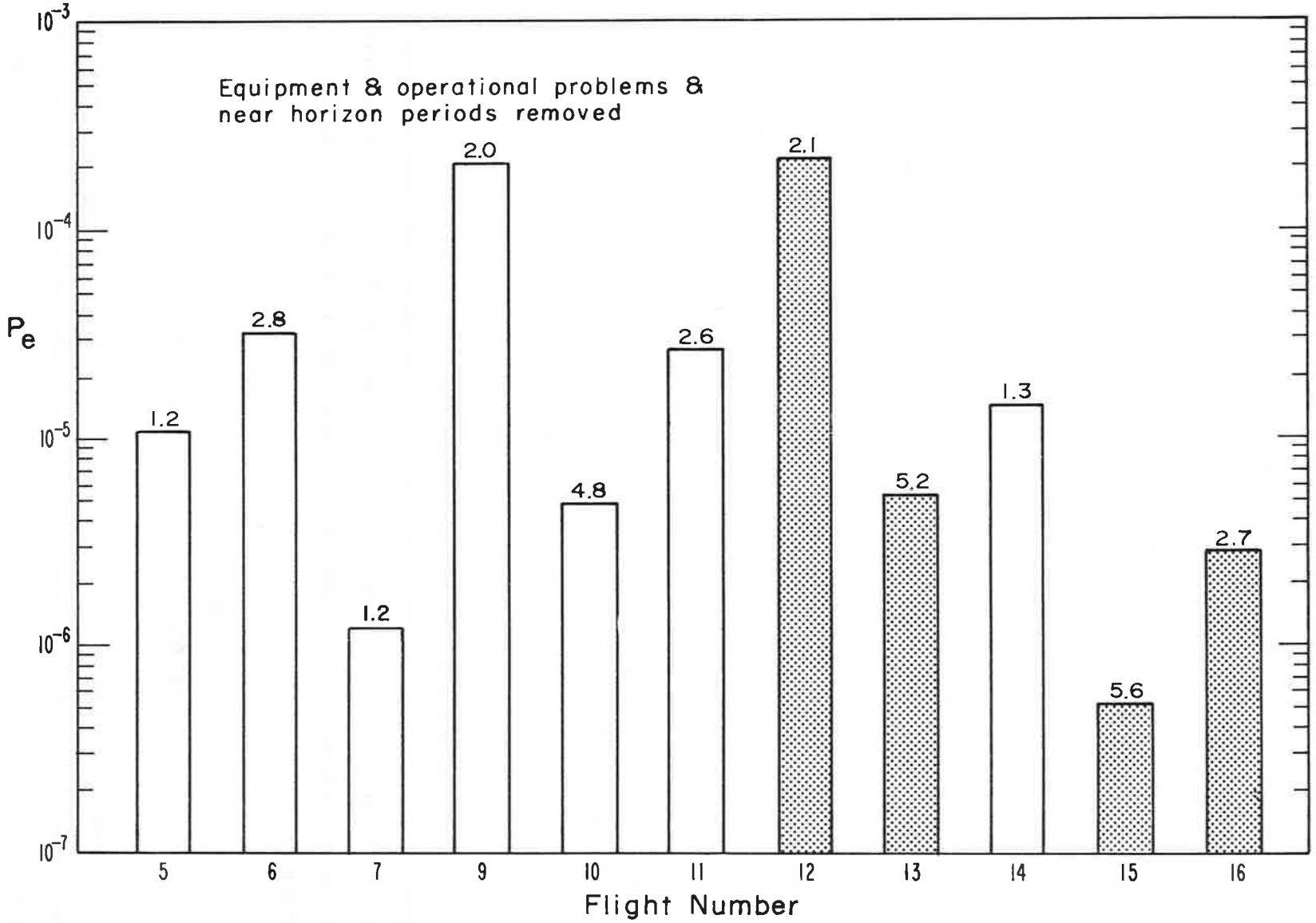

Figure 19. Average bit error rate for each flight removing equipment and operational problems and near horizon periods. Shaded areas denote 4800 bps flights.

The bit error rates for the tests are summarized by computing the averages for all 11 flights. This result is shown in figure 20 together with the averages of the 2400 and 4800 bps flights respectively. The figure shows the averages both before and after the various errors are removed. In summary, the average bit error rate removing equipment/operational problems and near horizon periods are as follows:

	Pe
ALL FLIGHTS	4.6×10^{-5}
2400 bps	4.1×10^{-5}
4800 bps	5.4×10^{-5}

Note that the average bit error rates for the 2400 and 4800 bps flights are quite similar. Thus, 4800 bps does not appear to offer any significant disadvantage over 2400 bps in terms of error rate.

The averages shown in figure 20 are unweighted in that all flights are treated equally, regardless of their duration. Some reasoning can be forwarded that would support averaging on a "weighted basis" according to each flight's duration. This means that shorter flights will have a proportionally smaller effect on the average bit error rate computations than the longer ones. As a verification of this, we recomputed the average bit error rates using weighted averages, according to the formula

$$P_e = \sum_{i=1}^{N} P_i t_i \Big/ \sum_{i=1}^{N} t_i \quad , \tag{7}$$

where P_i is the probability of bit error for the i-th flight, t_i is the time duration during which P_i is measured, and N is the number of samples to be averaged. Results of these computations are shown in figure 21. Generally, the averages increase with weighting. The average bit error rate with weighting is:

	Pe
ALL FLIGHTS	6.8×10^{-5}
2400 bps	5.5×10^{-5}
4800 bps	7.7×10^{-5} .

The number of errors collected during the tests are listed in table 3. The number in the raw data column is the total number of errors and includes all errors regardless of their origin. Each of the remaining three columns

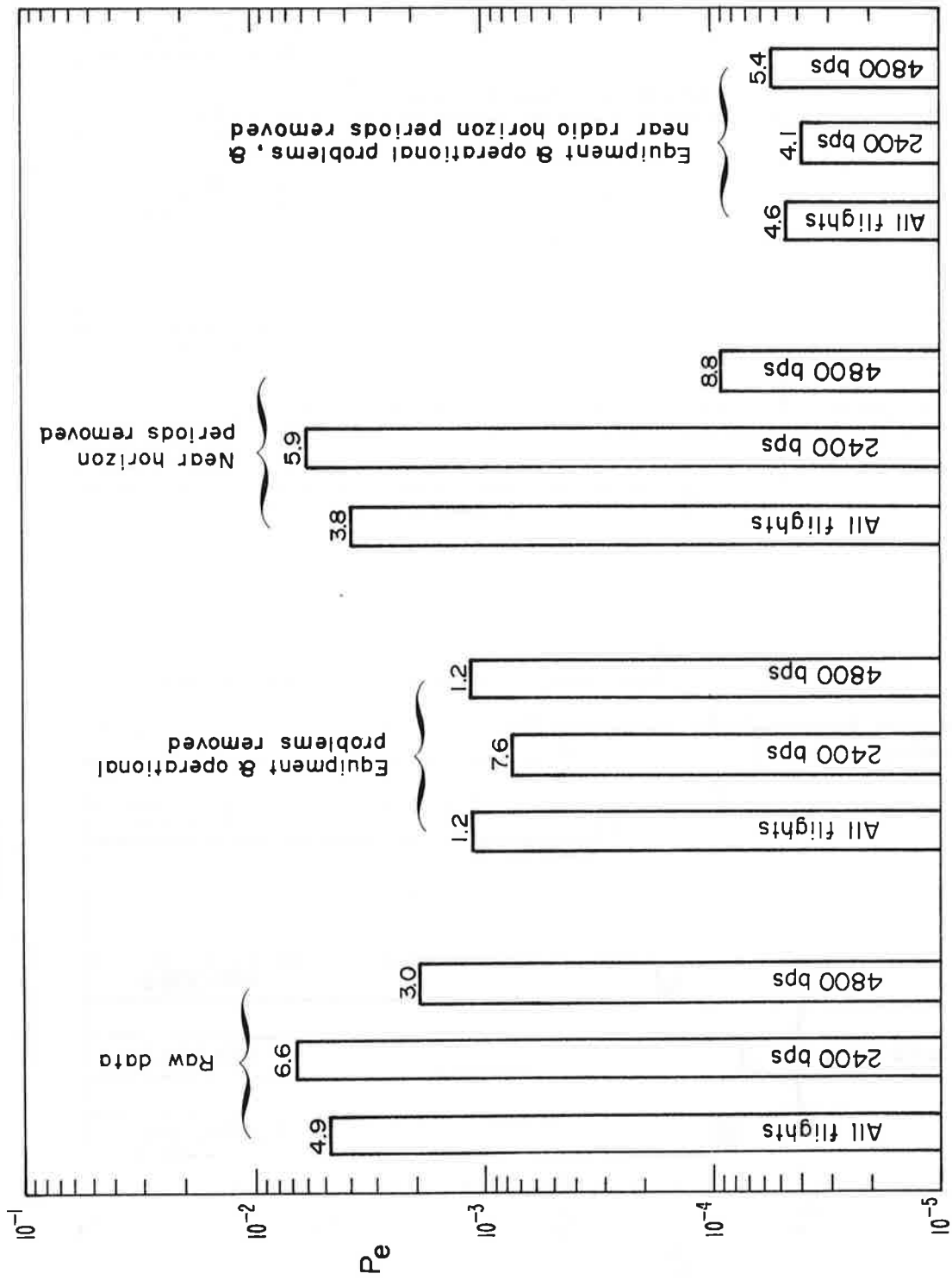

Figure 20. Summary of average bit error rate using unweighted averages.

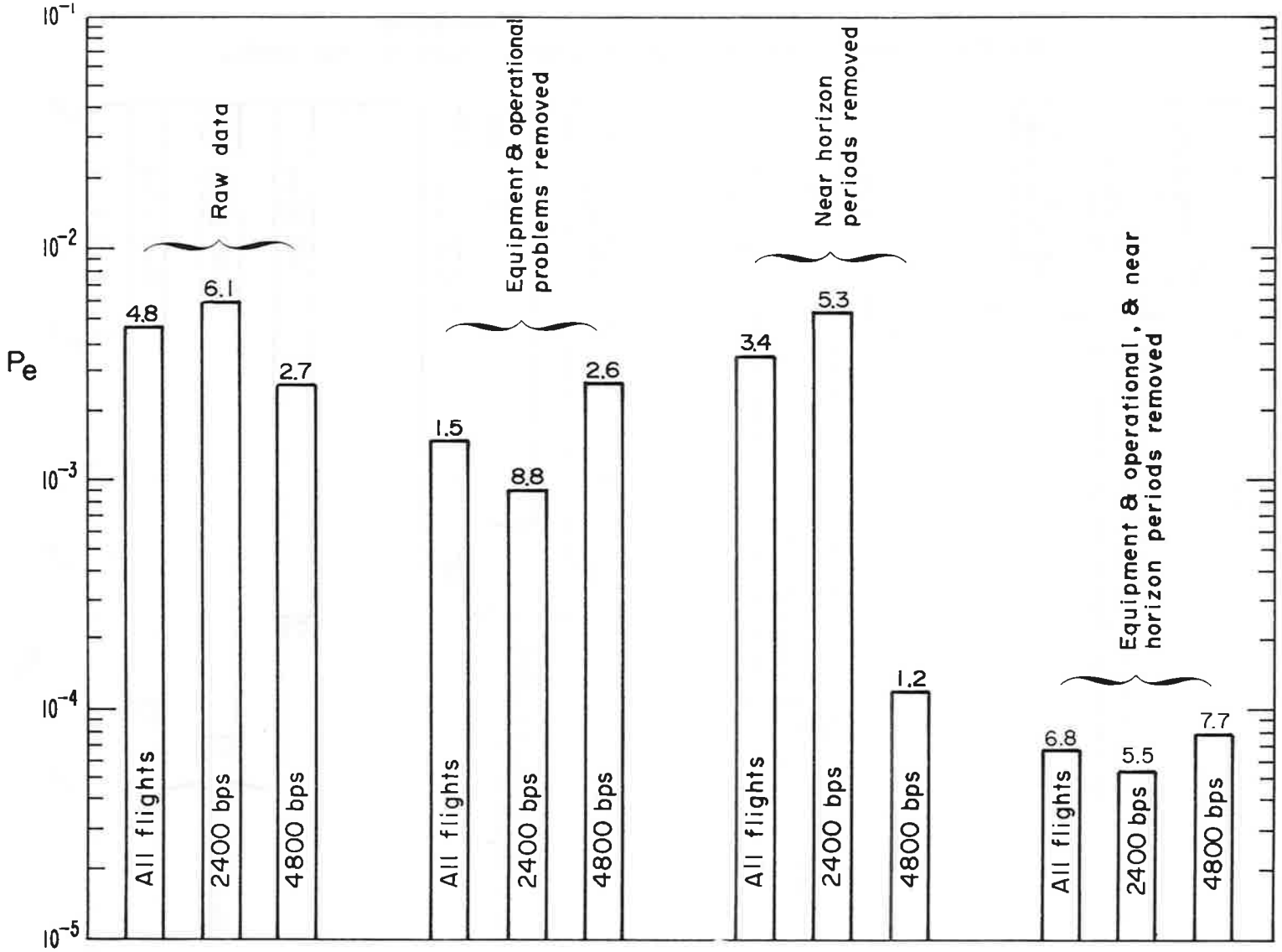

Figure 21. Summary of average bit error rate using weighted averages.

gives a breakdown of the source of these errors. These error counts are useful in assessing the accuracy of the bit error rate measurements.

Table 3. Number of Errors Collected During the Flights

Data Rate	Total Errors Raw Data	Total Errors Equip, Operational Problems	Total Errors Near Horizon Region	Total Errors Other Sources
2400	611751	523659	82690	5402
4800	308556	4832	294829	8895
	920307	528491	377519	14297

4.4 Measured Block Error Rate

In addition to bit errors, measurements are also made of block errors. The HP-1645A test set continuously counts block errors by dividing the incoming bit stream into 1000 bit blocks and recording a block error if one or more bits within the block are in error. The average block error rate for each flight using the raw data is shown in figure 22. Again, this includes all block errors regardless of origin. Figure 23 shows the results removing block errors caused by equipment, operational problems, and the near horizon region.

A summary of the block error rate is given in figure 24, where the average values are as follows:

	P_B
ALL FLIGHTS	1.6×10^{-2}
2400 bps	1.7×10^{-2}
4800 bps	1.4×10^{-2},

with the equipment, operational, and near horizon errors removed. Using these averages, the average number of bit errors per block error (N_B) can be calculated from

$$N_B = (P_e \times 1000)/P_B. \tag{8}$$

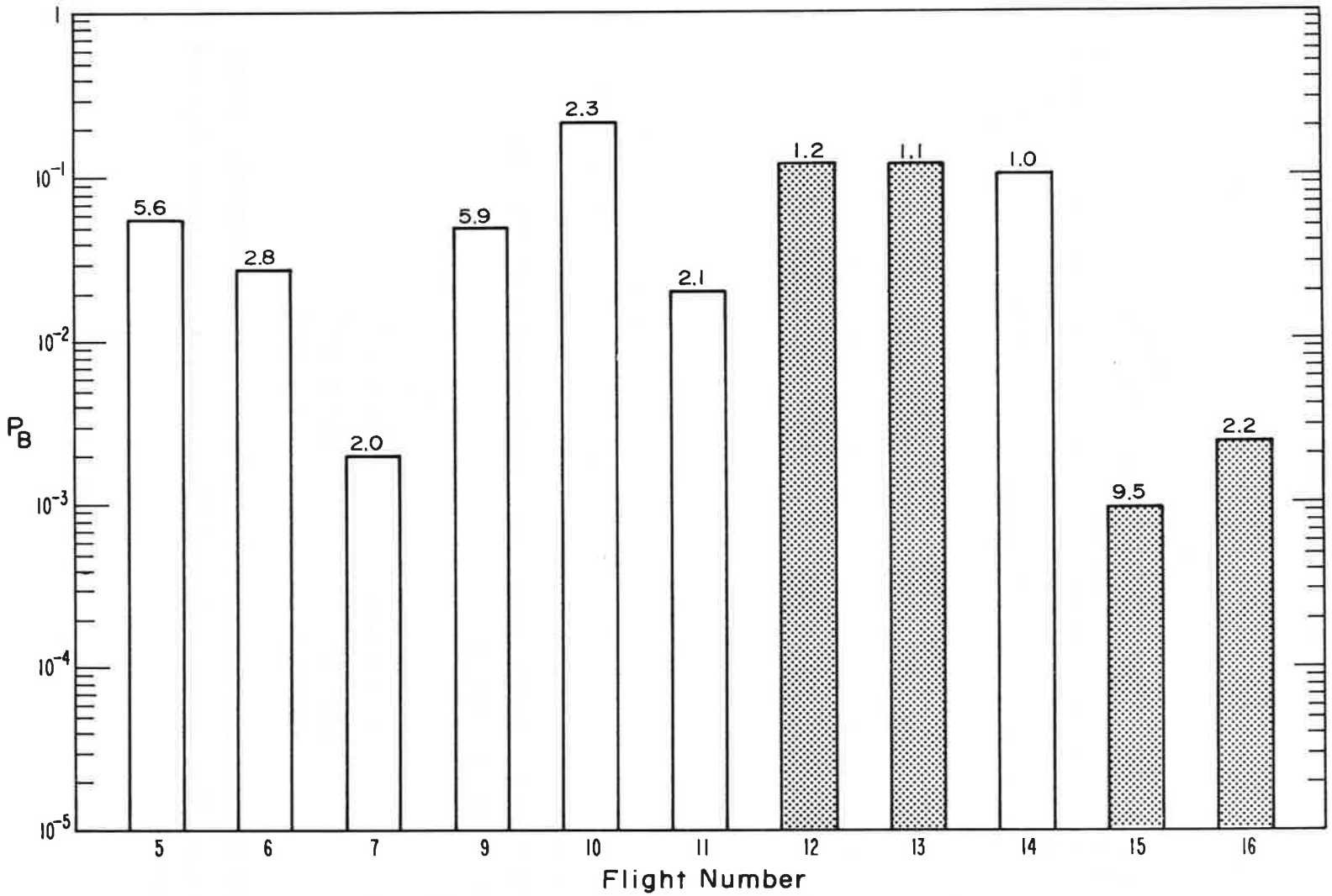

Figure 22. Block error rate for each flight using data as supplied by NAFEC. Includes errors due to equipment and operational problems. A block is 1000 bits.

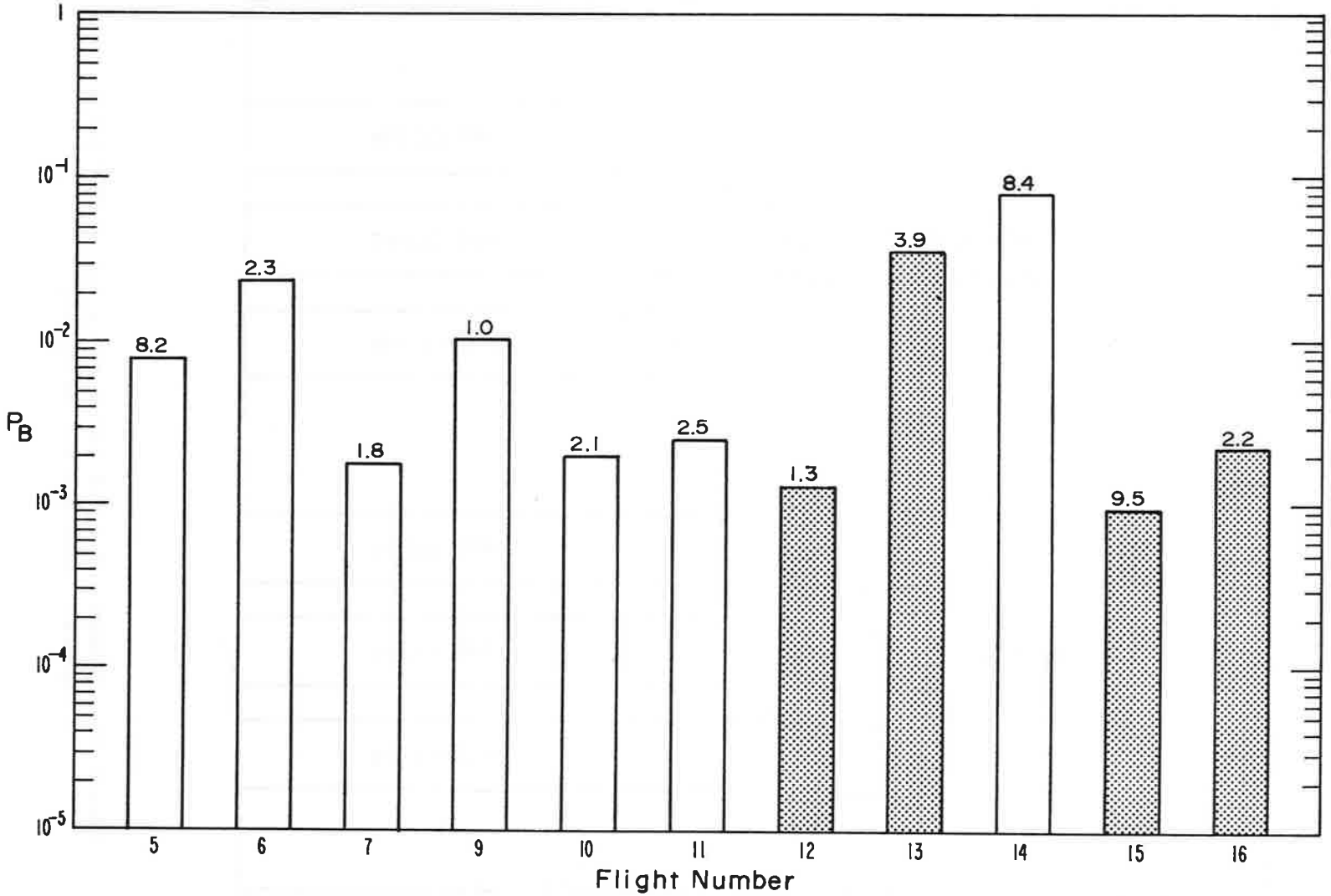

Figure 23. Block error rate for each flight removing equipment and operational problems and near horizon periods. A block is 1000 bits.

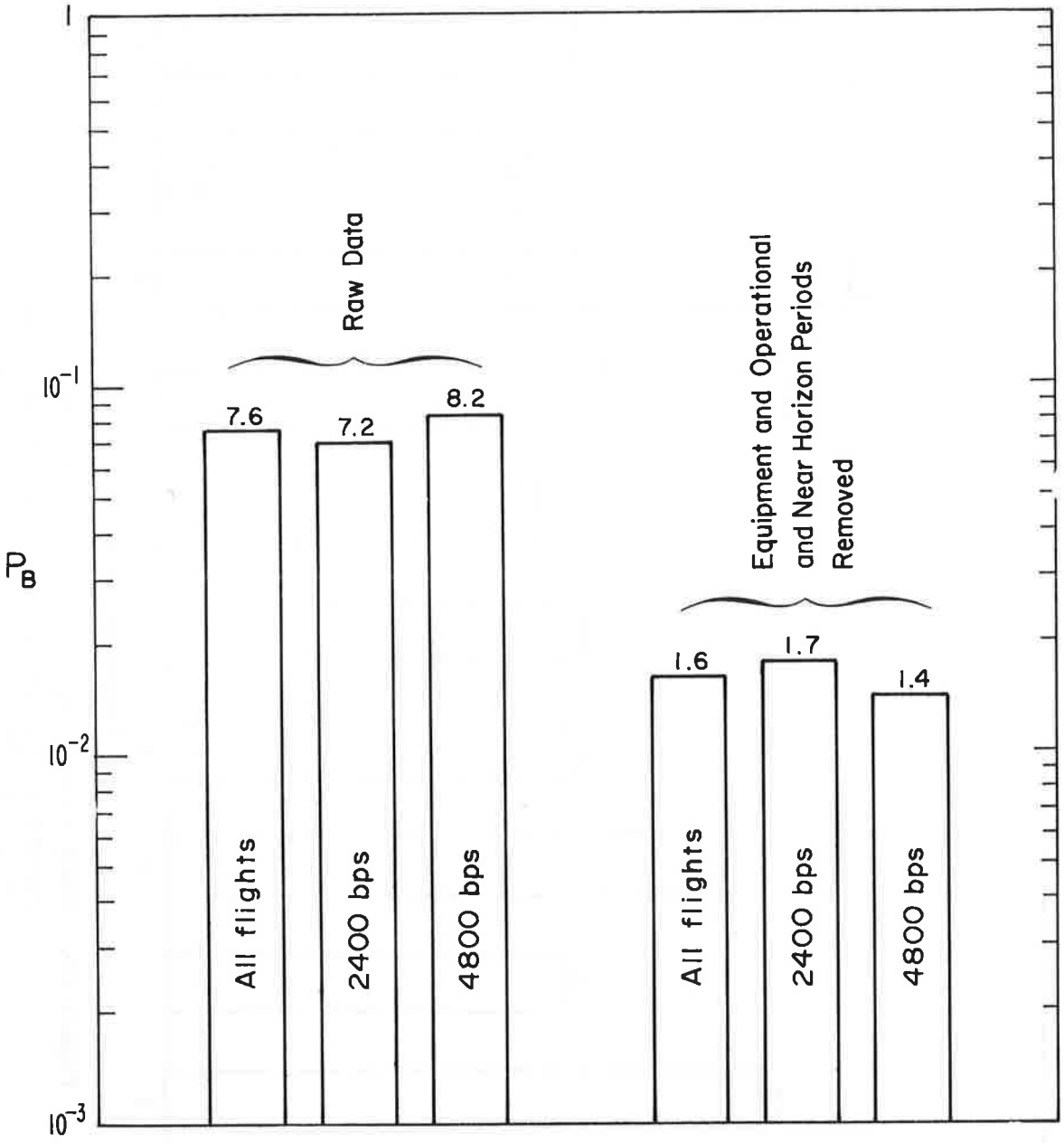

Figure 24. Summary of block error rates for a 1000 bit block. Averages are weighted.

The results are as shown:

	N_B
ALL FLIGHTS	2.9
2400 bps	2.4
4800 bps	3.9

The reader should be aware that this computation assumes that all bit errors are equally proportioned among all blocks with errors. If the errors are bunched, the results may be different. Fortunately, additional data are presented later in the report in order to substantiate the above computations.

The reader is cautioned regarding the interpretation of N_B. The units, as noted earlier, are in bit errors per block error. Thus, the quantity is really a measure of the average number of bit errors in a block given that a block has one or more errors. In other words, the average is made by examining only those blocks with one or more bit errors. Those blocks with no errors are not considered in the average.

4.5 Distribution of Errors

The magnetic tape recordings also enabled the data to be examined in 1 second samples. Thus, the data also can be examined in 1 second data blocks in addition to the 1000 bit data blocks as discussed in section 4.4, which provides an interesting insight into the data in larger size blocks.

To begin with, the number of bit errors per 1 second data sample was examined for all flights using the raw data. These results are shown in figure 25. The fractions were computed examining only those blocks with errors. Thus, after examining all 1 second data samples with errors, 18% of them had exactly 1 bit error, 7.3% had exactly 2 bit errors, etc. Since figure 25 contains both 2400 bps and 4800 bps data, the next step is to repeat the calculations using only the 2400 bps data as shown in figure 26. Similarly the results for 4800 bps are shown in figure 27. Generally, all three graphs appear to be similar. These calculations are for raw data and, therefore, include all errors regardless of origin. A comparison of the 2400 and 4800 bps data is shown in figure 28, where the end points of the histogram have been connected with solid or dashed lines for ease in comparison. Note that some

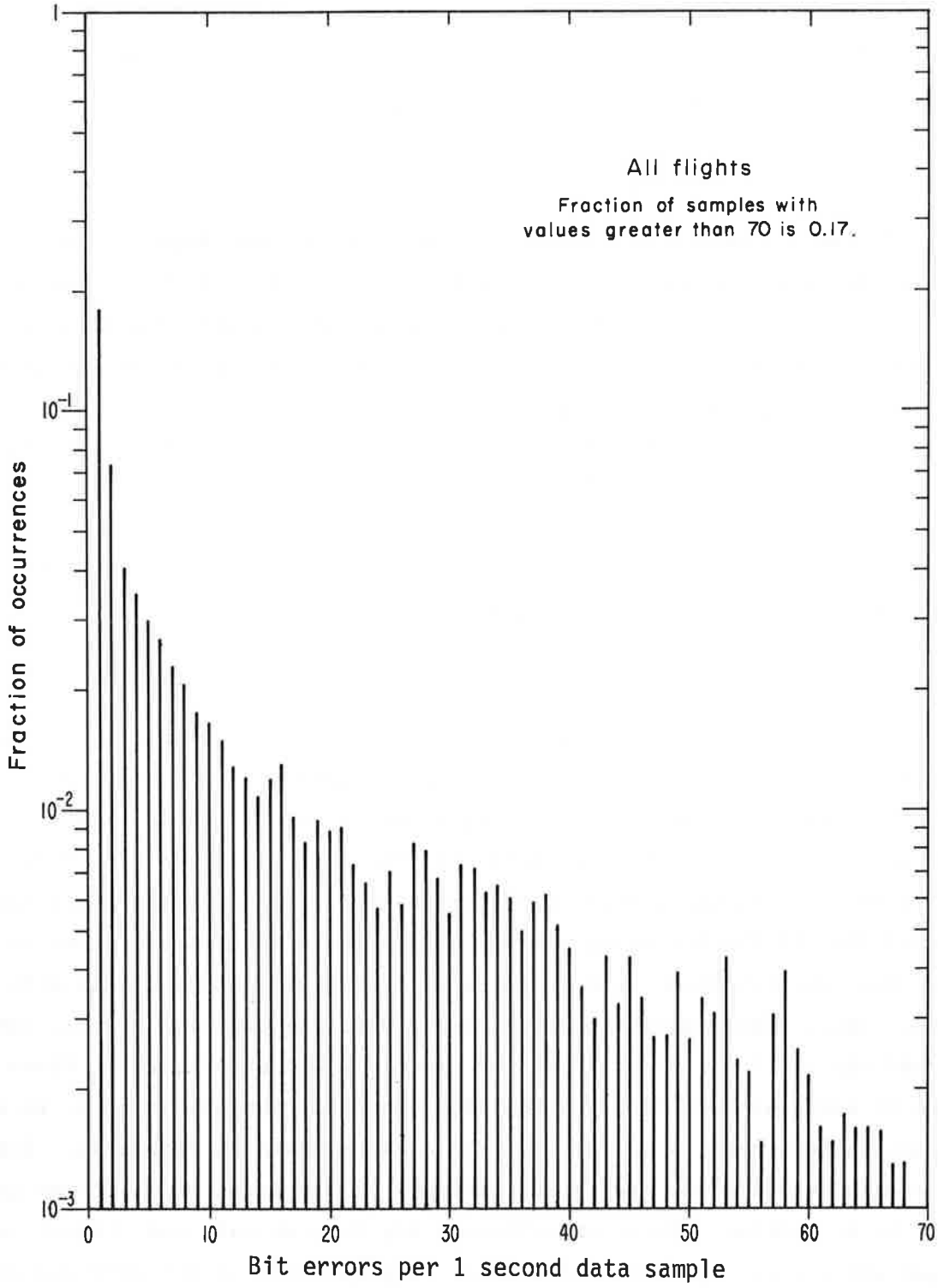

Figure 25. Histogram of number of bit errors per 1 second data sample for all flights using raw data as supplied by NAFEC.

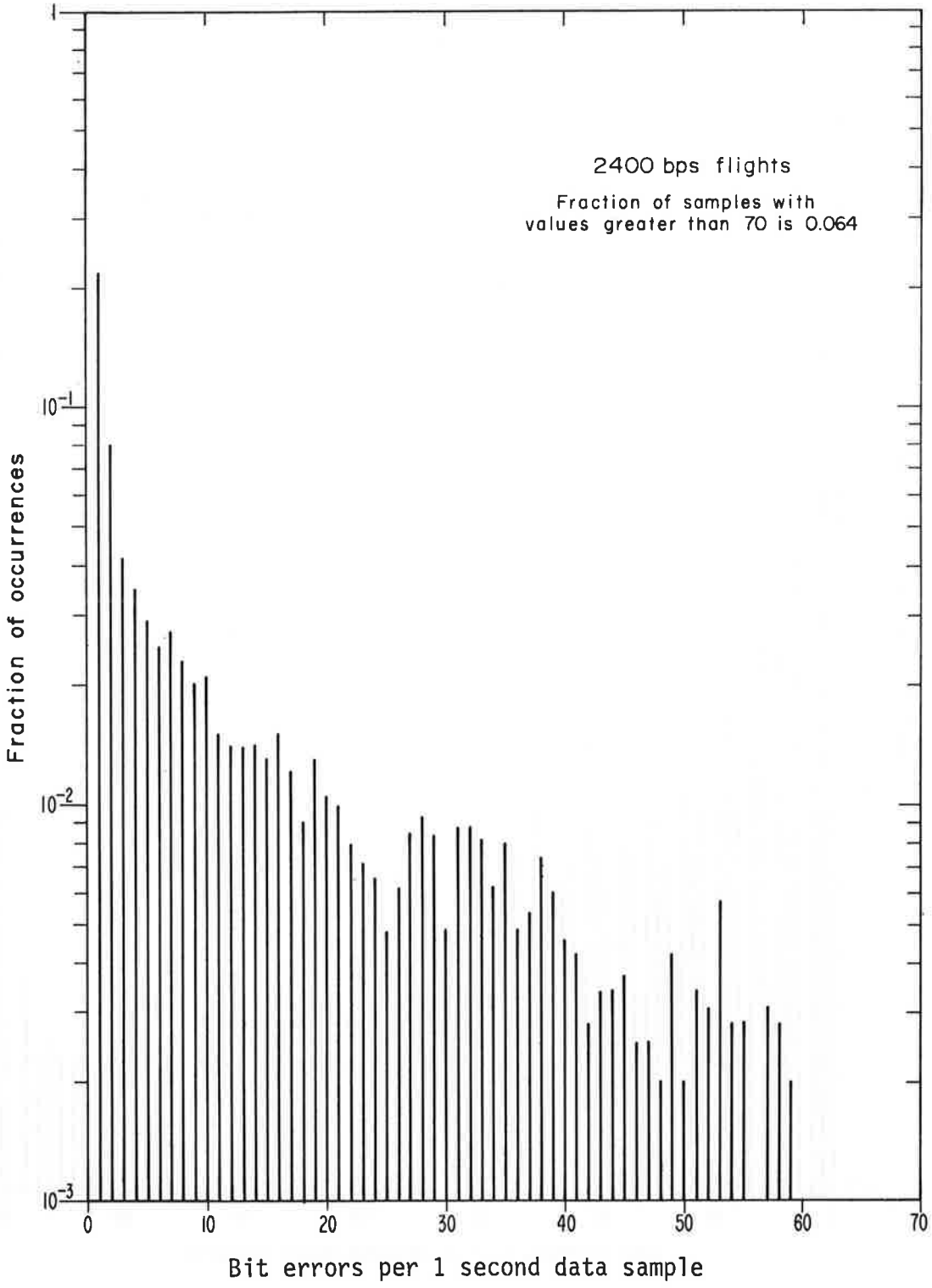

Figure 26. Histogram of number of bit errors per 1 second data sample for all 2400 bps flights using raw data as supplied by NAFEC.

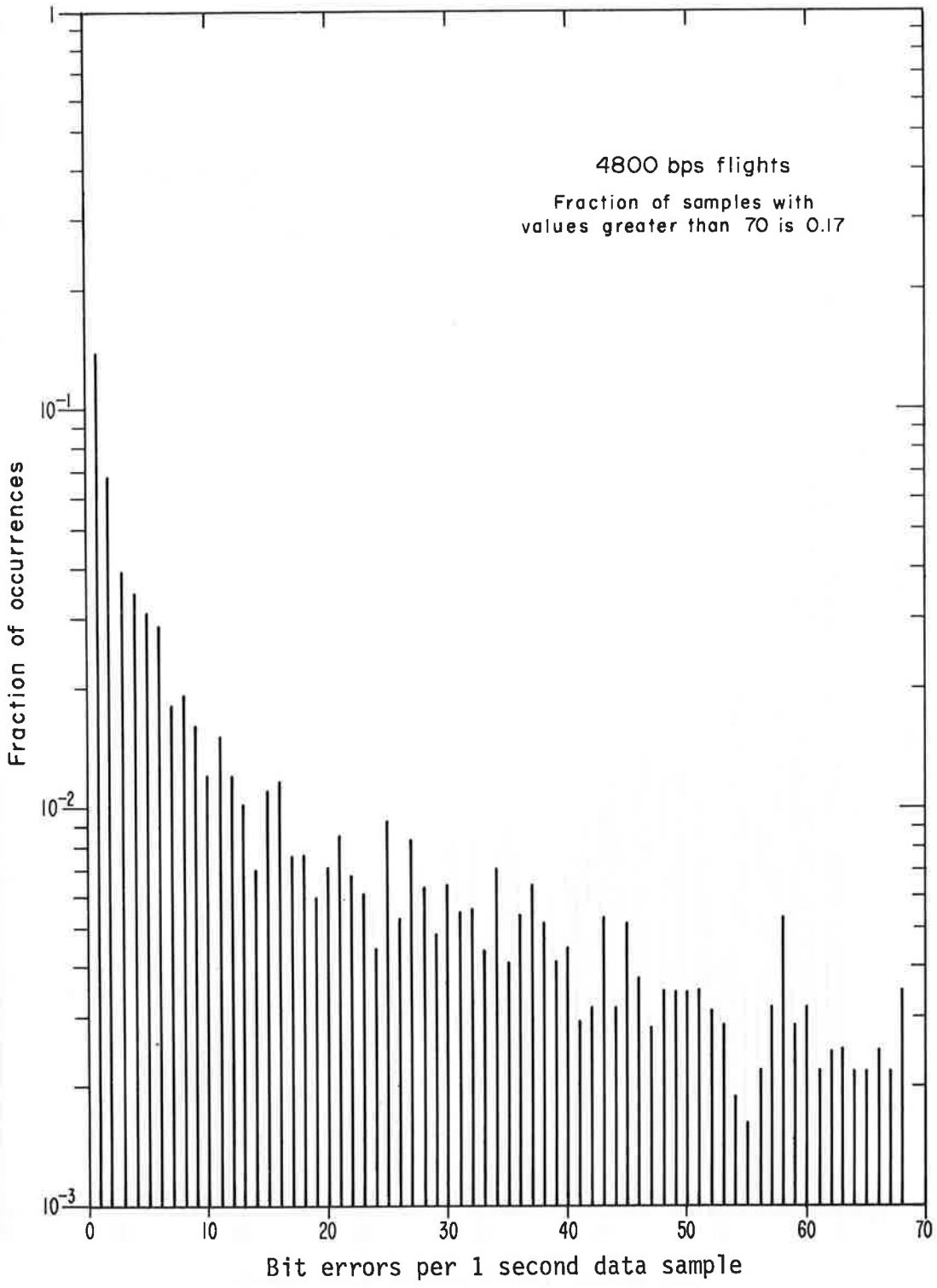

Figure 27. Histogram of number of bit errors per 1 second data sample for all 4800 bps flights using raw data as supplied by NAFEC.

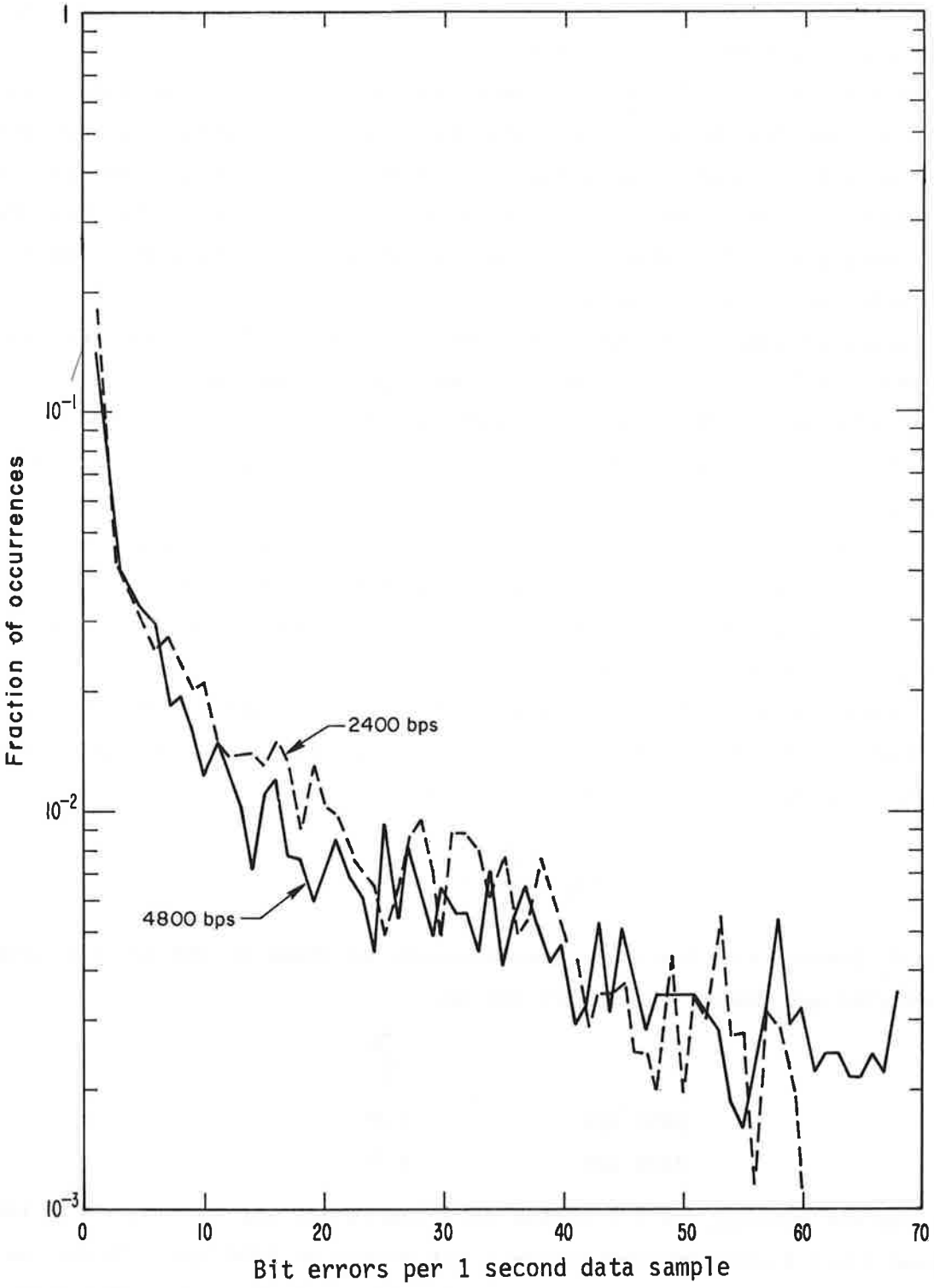

Figure 28. Comparison of the envelopes of the histograms that are shown in figures 26 and 27.

cyclic variation appears in the graphs that may indicate a slight clustering of the errors possibly due to fading.

So far, the calculations have been made with only the raw data and, therefore, are determined almost entirely by the near horizon periods when the error rate is high. Thus, the data do not reflect the greater part of the flight when relatively few block errors are encountered. The next two graphs were prepared to examine the distribution of errors during these relatively low error rate periods.

Figure 29 shows the distribution of errors for all 2400 bps flights removing near horizon errors and equipment/operational problems. This figure reflects the distribution of errors per 1 second data sample when the aircraft is well within line of sight. As expected, this distribution is distinctly different as 68% of the samples now have exactly 1 bit error. In fact, only 5% of the samples had more than 10 errors. Figure 30 is a similar plot for the 4800 bps data. The likelihood of having 1 or 2 bit errors is smaller at 4800 bps than at 2400 bps. However, the likelihood of 4 bit errors increases at 4800 bps.

A convenient check of the data can be made by computing the average number of bit errors per 1 second data sample in figures 29 and 30. This quantity will be denoted M_B and computed by

$$M_B = \sum_{i=1}^{\infty} i \cdot f_i , \tag{9}$$

where f_i denotes the fraction of occurrences as shown in the distributions. The results are, using figures 29 and 30,

	M_B
2400 bps	1.9
4800 bps	4.0 .

Thus, on the average, if a 1 second data sample has any errors, it is likely to have 2 bit errors at 2400 bps or 4 bit errors at 4800 bps. Again, we are averaging only those samples with errors. If we choose a 1 second data sample at random, it is likely to be error free. However, if it does have errors, it is likely to have M_B bit errors.

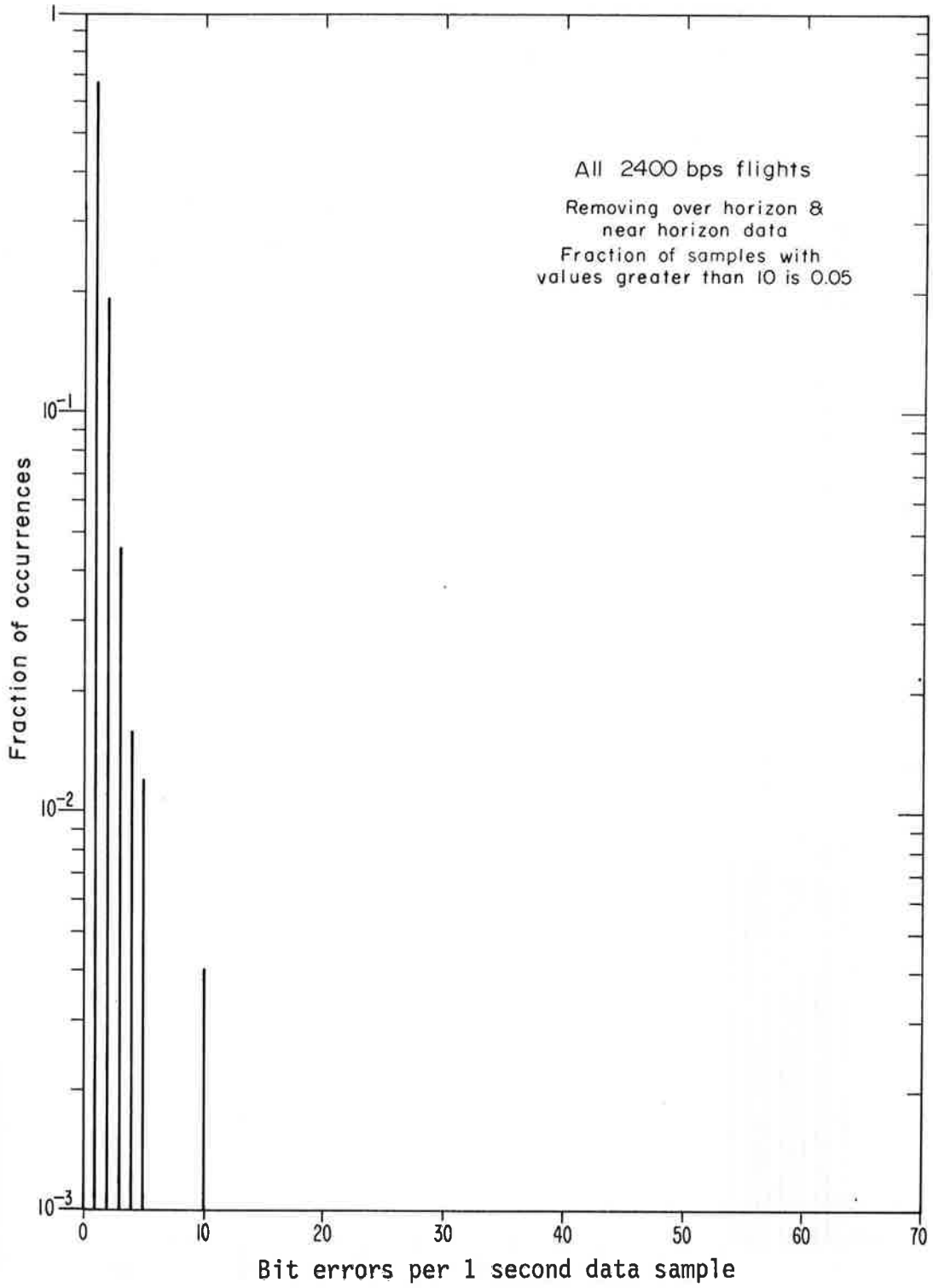

Figure 29. Histogram of number of bit errors per 1 second data sample for all 2400 bps flights removing equipment, operational, and near horizon errors.

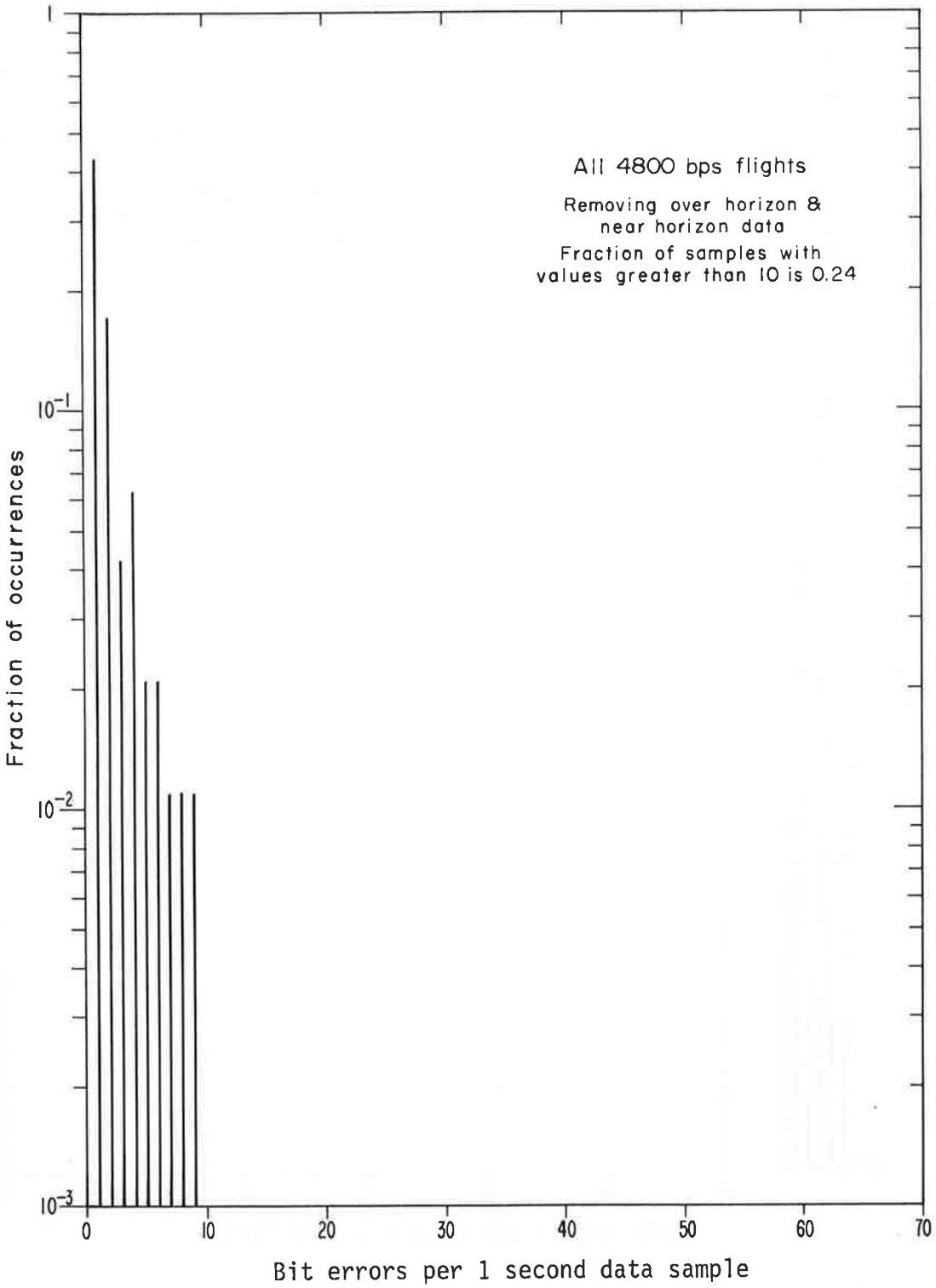

Figure 30. Histogram of number of bit errors per 1 second data sample for all 4800 bps flights removing equipment, operational, and near horizon errors.

Of course, M_B is quite similar to N_B. The only difference is that N_B is measured in a 1000 bit block while M_B is measured in 2400 or 4800 bit blocks, depending on the bit rate in use. Our measurements show that N_B is approximately equal to M_B which means that the average number of bit errors per block does not increase with increasing block size, at least over the range considered here. This is a reasonable conclusion and can be intuitively explained as follows.

Consider the diagram shown in figure 31. The probability of any 1000 bit block being in error is given by P_B. We have already seen that if a 1000 bit block has any errors, it is likely to have N_B bit errors in that block. If we arbitrarily extend the observation period to 2000 bits, it is very unlikely that we will encounter any additional bit errors due to the low block error rate. In fact, the probability of two consecutive blocks having errors assuming indpendence is $P_B \cdot P_B$ which is approximately 10^{-4} when the aircraft is well within line of sight. Thus, with modest increases in block size (1000-bit to 4800-bit block) we do not expect any significant increase in average number of bit errors per block.

We can summarize by stating that the average number of bit errors per block, given that the block has one or more errors, is 2 for the 2400 bps flights, and 4 for the 4800 bps flights. These figures are the same for both 1000 bit and 1 second blocks, and are with the equipment, operational, and near horizon errors removed. When the aircraft is in the near horizon region, the averages will be higher.

4.6 Near Horizon Region

Another result that can be obtained from the data is a measurement of the maximum usable range during the flights. As noted in figure 15, when the aircraft approaches the radio horizon, on an outbound flight, it first enters a region of increasing bit error rate. The error rate continues to increase until eventually the received signal level drops below the 2 μV minimum squelch threshold. At this point, the receiver turns off and a loss of carrier is noted at the receive modem. The data test set is disabled and no bit or block errors accrue until the aircraft returns into a usable signal area.

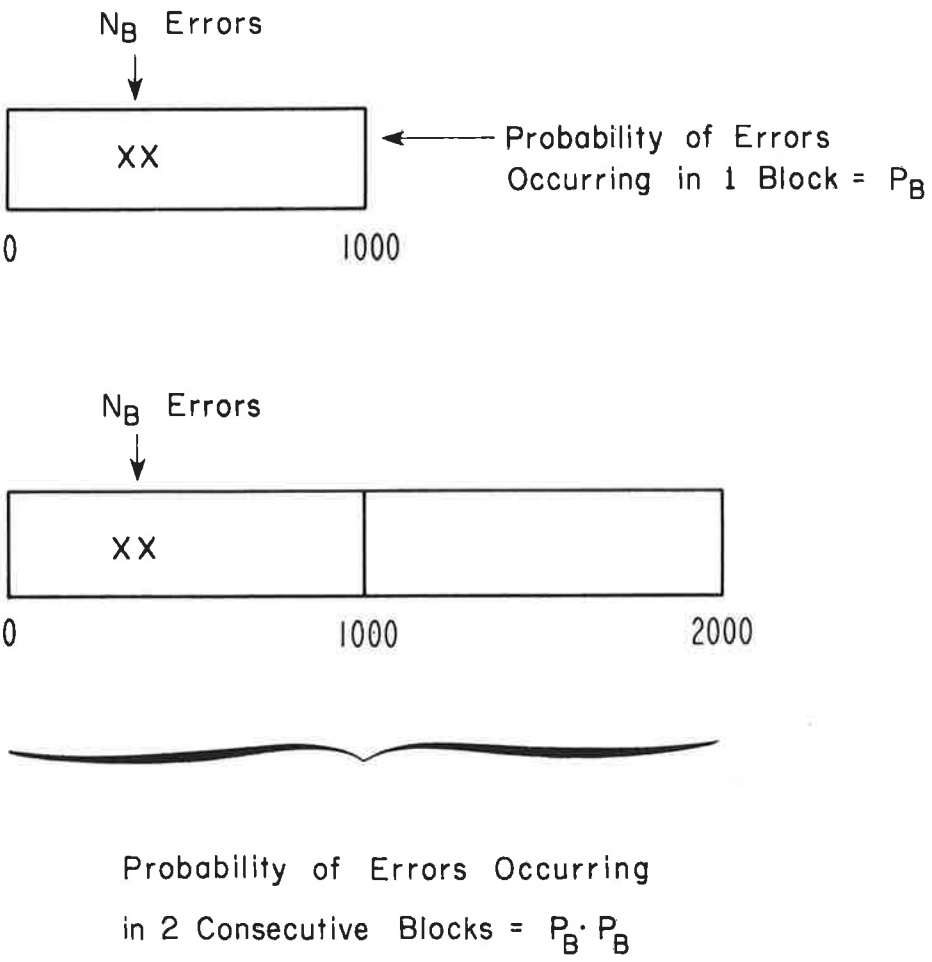

Figure 31. Description of occurrence of block errors.

Generally, during a flight, the test aircraft traveled well beyond the radio horizon. On the return flight, the first thing that generally occurs is that the receiver squelch enables and the modem begins to receive signal. The bit and block error rate, at this point in time, is high, and clock slip and carrier loss indications are frequently noted. As the aircraft continues toward the ground site, eventually the error rate stabilizes and remains relatively constant.

The region of high error rate just prior to loss of sync and immediately after regaining sync is called the near horizon region and is generally a region of poor reliability. A graph of this region as a function of altitude and slant range is shown in figure 32. All outbound flights with loss-of-sync are shown by lines with arrows. The lines indicate the high error rate region and the arrowheads indicate where the loss of sync occurred. Similarly, the return condition is shown with circles and straight lines. A circle indicates the point where the signal first returns, and the solid line indicates the high error rate region.

As a check of these measurements, the ITS propagation model was used to predict propagation loss under similar conditions [Gierhart and Johnson, 1973 . Resulting predictions for 5% and 95% availability and 140 dB loss are also shown on figure 32. Thus, 90% of the time, one should expect the 140 dB propagation loss to occur within the two boundaries.

A 140 dB propagation loss will result in a signal at the ground receiver of approximately 3.5 μV, again assuming 0 dB for the combined losses and gains as given in (3). Out of the 34 near horizon samples examined, 30 were either entirely or partially within the two bounds. The predictions were made using a terrain variability factor of zero (smooth earth).

Three of the samples showed near horizon regions beyond the predictions while one sample was less than predicted. These four cases were encountered during flights 5, 11, and 14, which were all New York flights, largely over water. Possibly, over-water propagation anomalies have some bearing on these flights.

The width of the near horizon region, ΔD, is another parameter that can be deduced from the data. A graph of ΔD as a function of altitude is shown in figure 33. As can be seen, the width of the near horizon region varies anywhere between 0.5 and 21 n mi with an average width of 10 n mi.

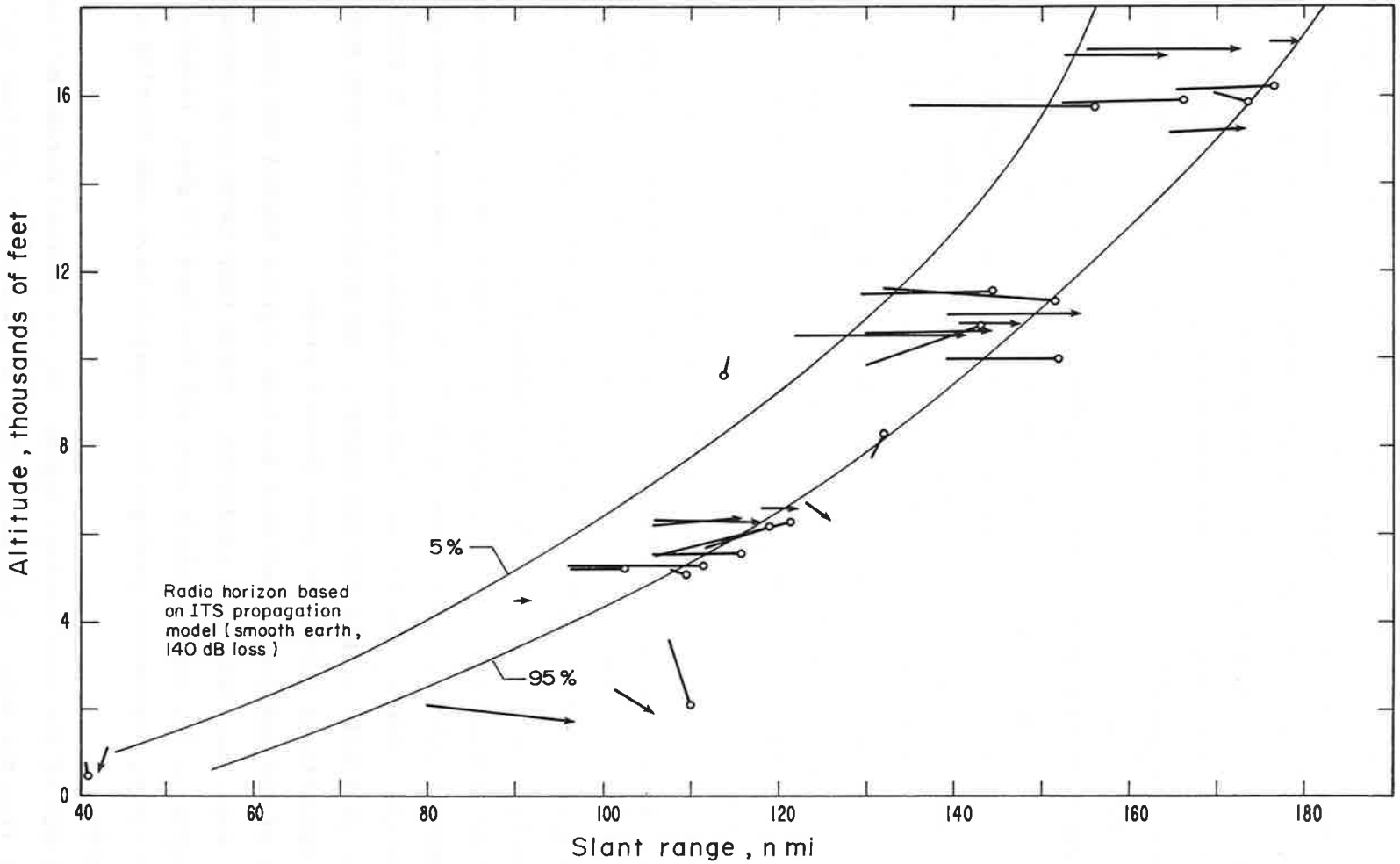

Figure 32. High error rate regions as a function of altitude and slant range. Arrows indicate loss of sync on outbound flights. Circles indicate re-establishing sync on inbound flights.

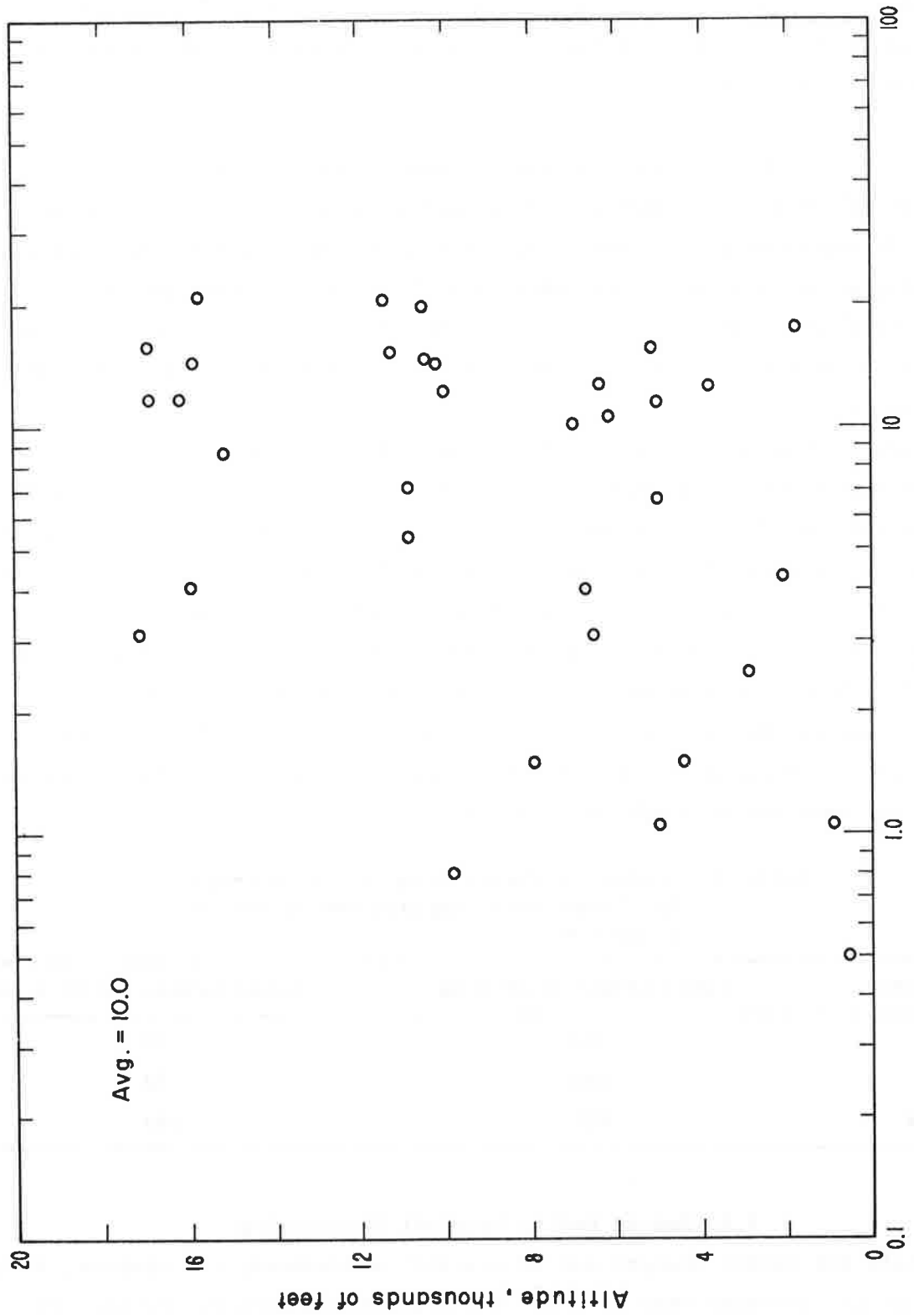

Figure 33. Width of near horizon region as a function of aircraft altitude.

Generally, ΔD appears to be independent of altitude, and probably is a function of a combination of factors such as direction of travel relative to ground site and aircraft attitude.

4.7 Bit Errors During Takeoff and Landing

One of the problems noted earlier in the report is the increase in signal fading during the takeoff and landing periods. The aircraft is also generally performing additional maneuvers during this period which can result in signal fading. In order to see to what extent this is reflected in the data, we have analyzed the bit error rate as a function of aircraft distance from the ground site.

Figure 34 shows the average bit error rate when the aircraft slant range is 0-20 and 20-40 n mi from the ground site. The number of errors that were used in the calculations is shown in table 4. All equipment errors and near horizon periods have been removed in these calculations. A decrease in bit error rate can be seen as the aircraft moves away from the ground site. Approximately one order of magnitude difference exists between the bit error rate at 0-20 n mi as compared to 20-40 n mi out. This difference is probably due to the increased fading when the aircraft is close to the ground site. Thus, it would appear that a modest increase in bit error rate does occur when the aircraft is close in.

Table 4. Number of Errors Used in the Average Bit Error Rate Computations Shown in Figure 34.

Data Rate	Total Errors 0-20 n mi	Total Errors 20-40 n mi
2400	353	72
4800	168	72
Total	521	144

4.8 Fading During Aircraft Maneuvering

While the signal changes due to aircraft maneuvering are obvious, it is difficult to correlate them with any one aircraft parameter. Rather, it appears that signal fading during maneuvering is a complex function of pitch,

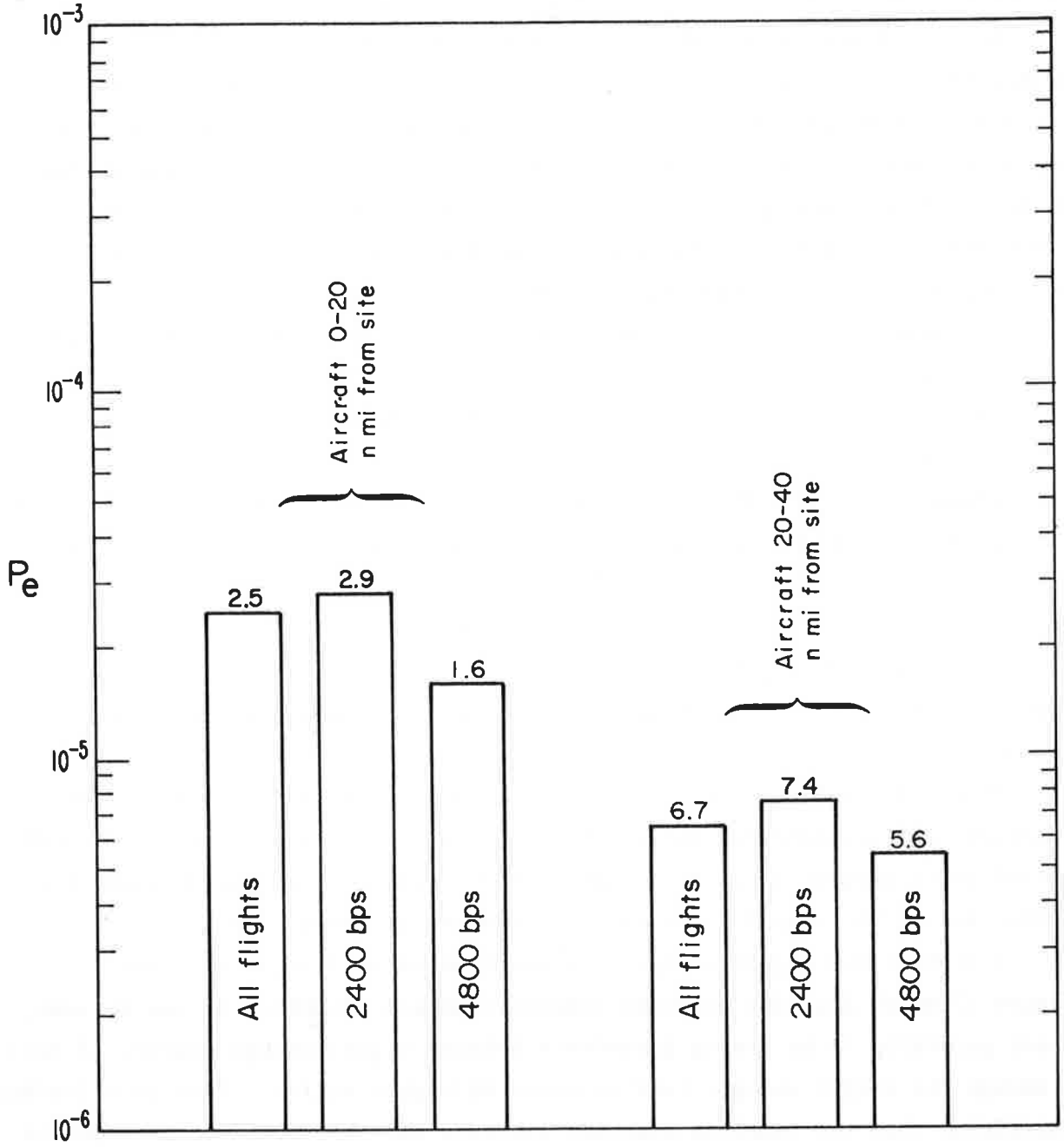

Figure 34. Average bit error rate as a function of aircraft distance from site. Equipment, operational, and near horizon periods have been removed.

roll, and yaw relative to the receiver. In this section of the report, some of the relevant observations on fading are described.

The first measurement described in figure 35 is the maximum signal change that occurs due to aircraft maneuvering on each flight. Generally, the maneuvers result in a signal fade that is denoted with a negative number. A positive number indicates a signal increase, as measured from the average of quiescent condition, that is due to the cyclic variation during spiraling maneuvers. The values denote peak signal changes as measured from the average value just prior to the maneuver.

An example of the fading structure during an aircraft spiral is shown in figure 36 where both roll angle and received signal level are plotted as a function of aircraft heading. Three complete aircraft spirals are shown on this graph. At an aircraft heading of 220^{o}, the aircraft is facing toward the ground site and at 40^{o}, it is facing away from the ground site. Note the repeatability of the signal during each orbit. Four distinct "nulls" occur during each orbit that are attributed to the aircraft antenna pattern. The increase in average signal strength is curious since the aircraft's slant range is relatively constant. This increase is probably due to the fact that the aircraft's altitude is increasing and that it is also near the radio horizon.

It is also interesting to examine the bit errors during this maneuver. No errors are recorded during the spirals shown in figure 30 until the middle spiral where a burst of 96 and a burst of 45 errors are recorded during the sudden roll. The signal level is also changing at those times.

A plot of the signal change as a function of roll angle is shown in figure 37 which includes selected samples from all flights. As can be seen, there generally is no strong dependence between signal change degrees of roll although the larger changes tend to occur at higher angles. This is a further indication that the complete aircraft attitude must be looked at in order to determine signal change during aircraft maneuvers.

4.9 Carrier Loss and Clock Slips

One of the parameters continuously recorded is a count of carrier loss and clock slips for each flight. The presence or absence of a carrier is determined at the MSK modem, which then sends a carrier status indication to

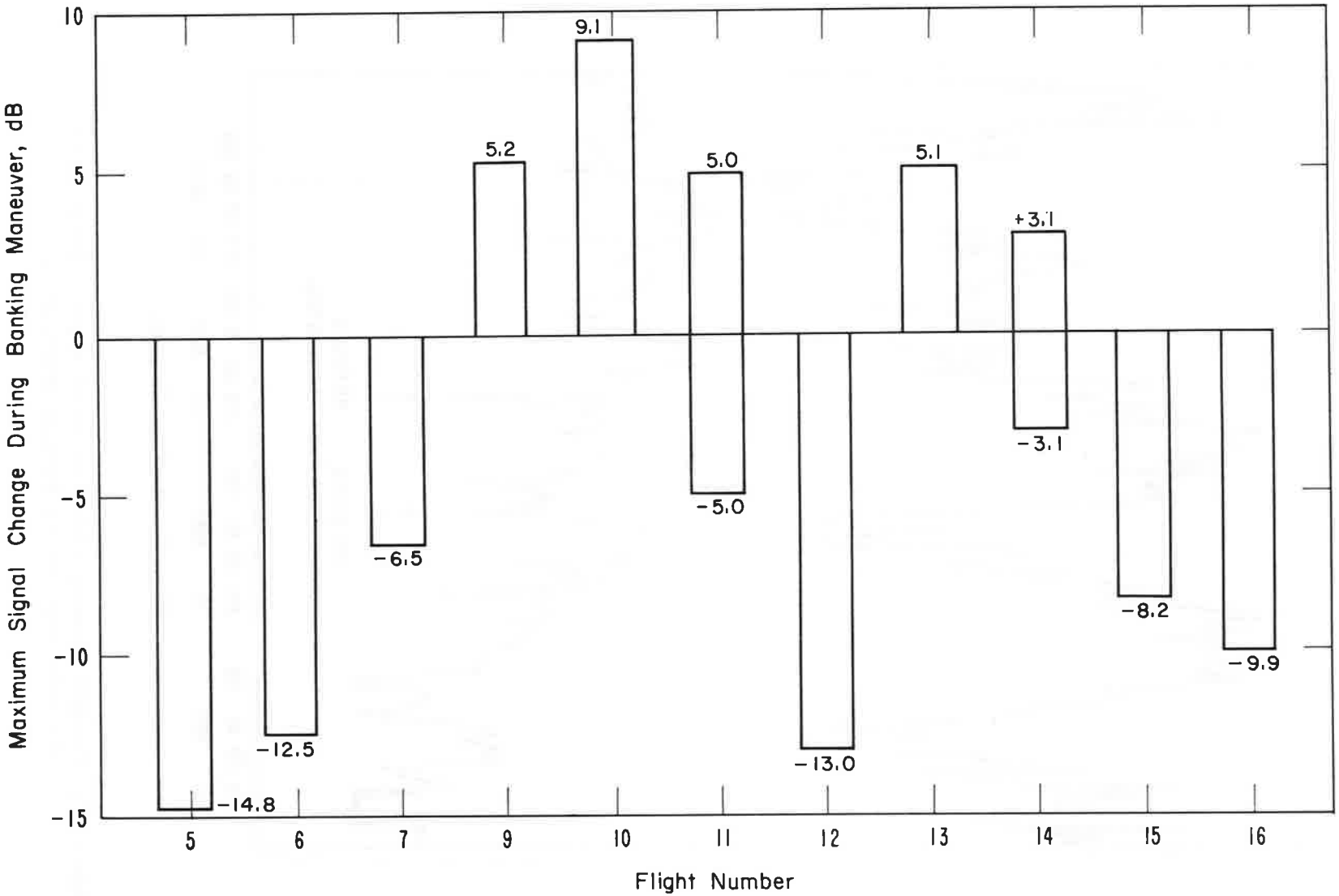

Figure 35. Maximum signal change from average due to aircraft banking maneuvers.

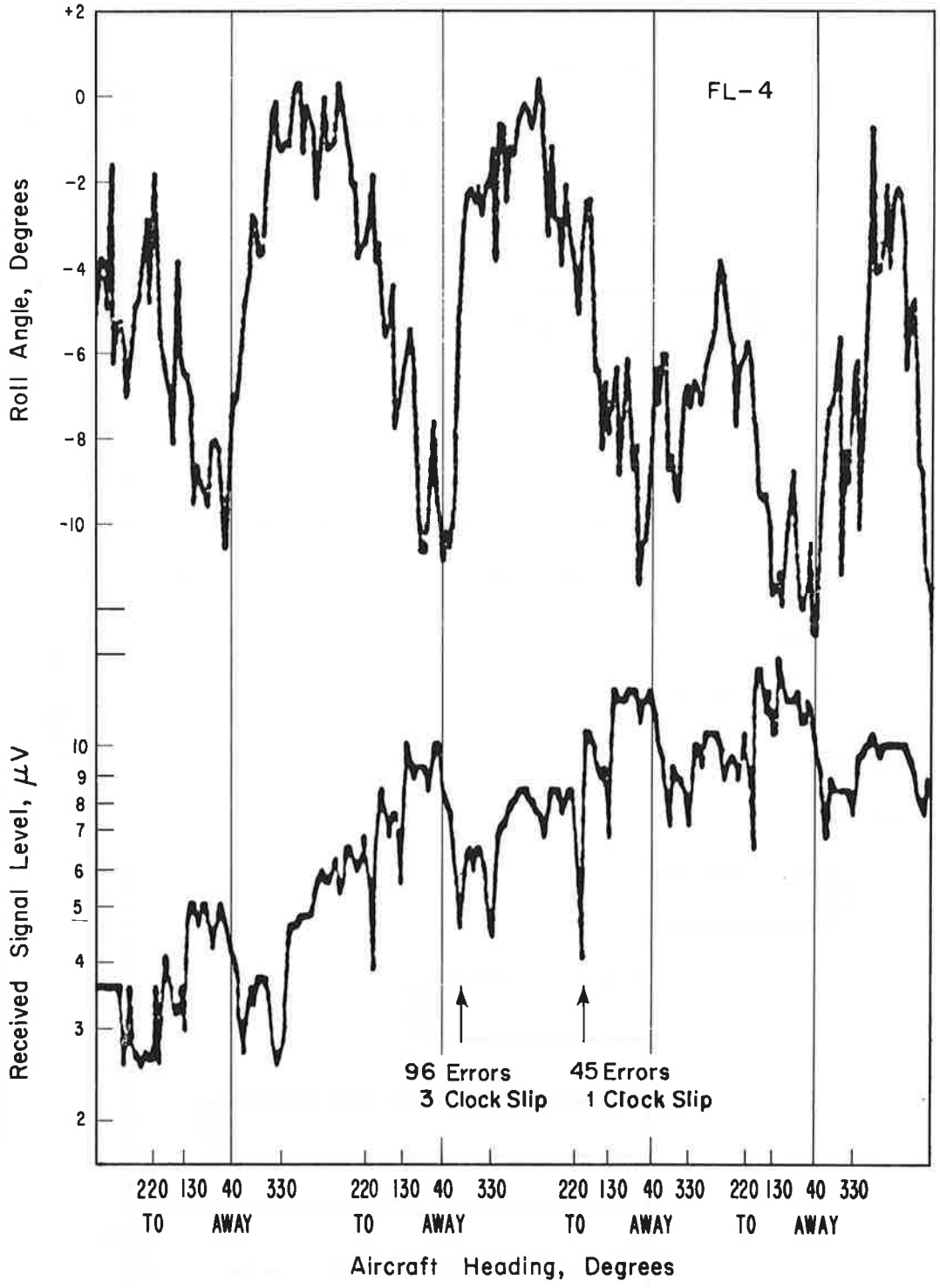

Figure 36. Example showing correlation of signal change with aircraft roll during banking maneuvers.

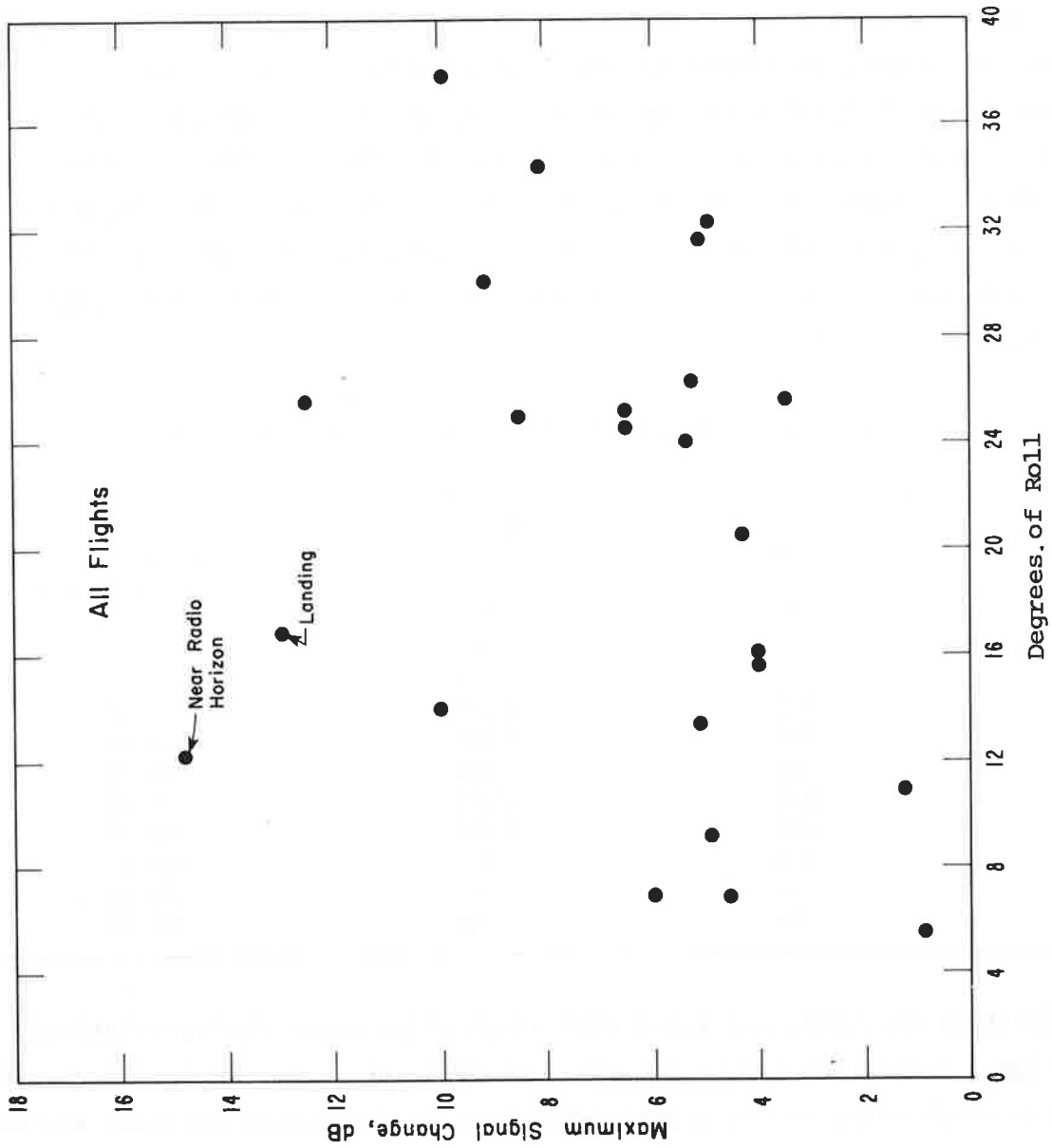

Figure 37: Maximum signal change as a function of degrees of roll.

the data test set that counts the number of changes. Clock slips, on the other hand, are determined by the data test set and are an indication of incorrect bit synchronization.

A list of the total count of clock slips and carrier losses for each flight is given in Table 5. The maximum occurs during flight 12 with 928 clock slips and 1892 carrier losses. However, all of the clock slip and carrier loss counts in flight 12 can be attributed to weak signals. The maximum received signal level in Table 5 denotes the maximum level at which any clock slips or carrier losses are observed. These problems almost always occur when the signal is less than 5 μV. Generally, clock slips happen after a signal outage when the receive modem is re-establishing sync. Although clock slips and carrier losses are primarily caused by poor signal conditions, a few exceptions do occur.

Table 5. Summary of Clock Slip and Carrier Loss Counts.

Flight	Clock Slips	Carrier Losses	Max Rec Signal Level
5	40	106	5 μV
6	38	41	5 μV
7	0	0	----
9	572	1136	5 μV
10	326	1245	5 μV
11	58	108	30 μV
12	928	1892	5 μV
13	642	1164	60 μV
14	353	757	200 μV
15	6	12	70 μV
16	29	38	60 μV

Thirteen occasions are noted when clock slips occur during relatively good signal conditions (10 to 200 μV). No apparent cause can be attributed to these clock slips as the signal appears to be relatively constant and no excessive aircraft maneuvering is noted. A typical example is shown in figure 38 where three periods of sync problems are shown during flight 15. The first clock slip occurs when the aircraft is near the radio horizon, where the signal is rapidly changing. The second occasion, however, consists of three clock slips that occur during relatively stable conditions. Neither

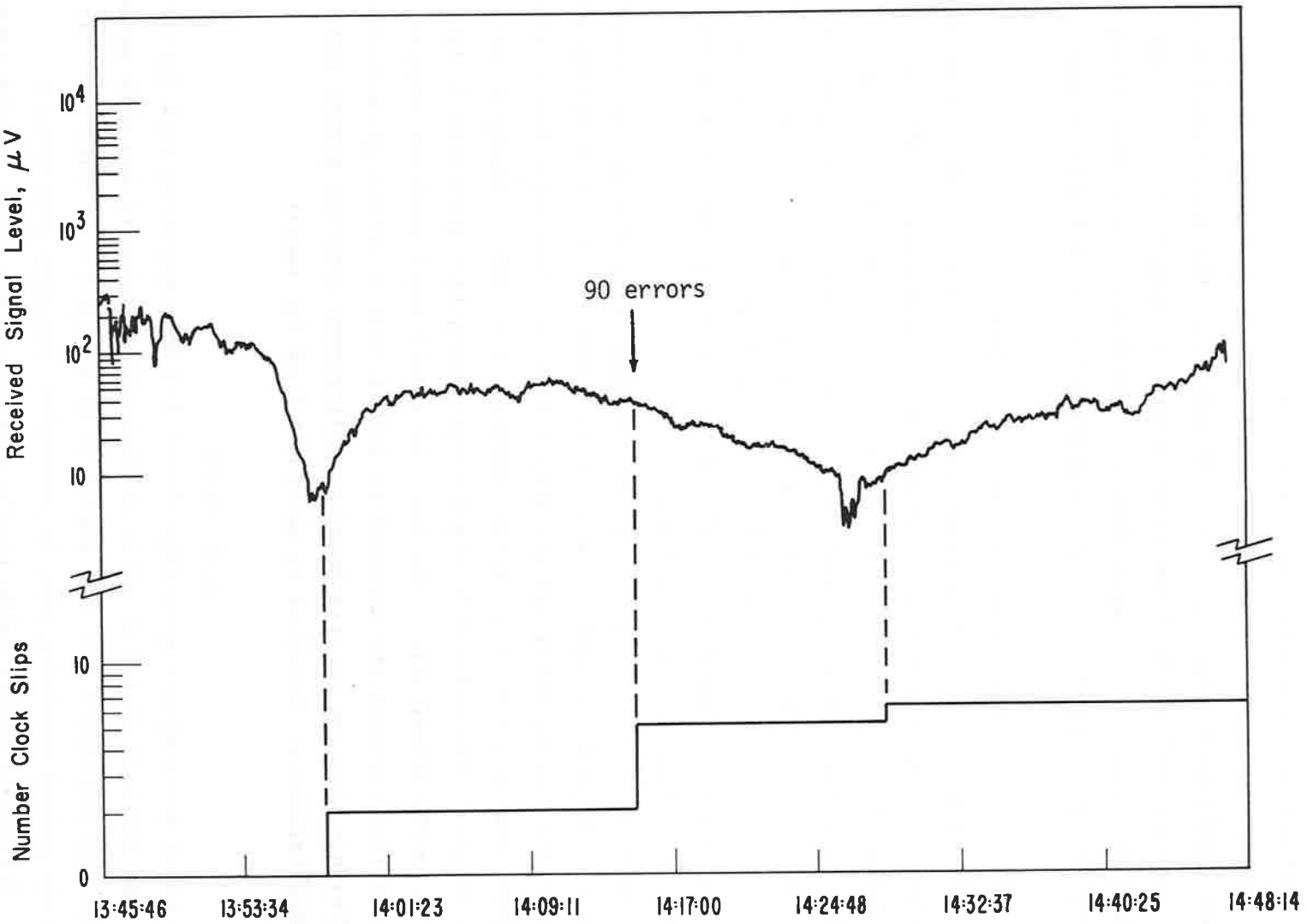

Figure 38. Example of flight where a clock slip occurred during a good signal condition.

excessive signal change nor aircraft maneuvering is noted at the time. However, a burst of 90 bit errors does occur simultaneously. The third clock slip also occurs in relatively good signal conditions.

In conclusion, a few periods were examined with clock slips during relatively good signal conditions. No apparent cause has been linked to the problem; however, relatively large error bursts, typically 100 bits, can occur simultaneously. It is impossible to determine from the data whether the errors are truly errors or simply a perturbation in the data stream.

4.10 Repeatability of Flights

While no extensive effort was made to measure the repeatability of the data, flights 15 and 16 offer some insight into repeatability. The two flights followed nearly identical flight paths with flight 16 originating 20 minutes after the return of flight 15. A plot of the altitude profile and received signal level, as a function of time, is shown in figure 39. The two scales on the left are relative in that they do not aline with either traces. The reference point of 125 μV and 6400 ft are denoted on each trace that can be used for alinement purposes.

As can be seen, the altitude profiles are nearly identical. The ground tracks of the flights are within 3 n mi of each other with the exception of the takeoff and landing which are slightly different. Note that the received signal level during the 8- to 54-minute section of flight is nearly identical for both flights. The aircraft's slant range during this period is 30 to 132 n mi from the ground site. The received signal level profiles seem to differ significantly when the aircraft is within 30 n mi of the ground site. This difference also can be attributed to reflections from the ground and surrounding terrain as described in section 4.2 of the report.

4.11 Noise

The noise measurements generally showed little correlation with the bit errors. The dominant source of noise at these frequencies is man-made noise. Automobile ignition noise does not appear to be a significant factor in the tests as the ground receiving site is reasonably isolated from vehicle traffic. Occasional strong noise impulses, however, are noted. While some isolated cases could be found where these impulses coincided with error

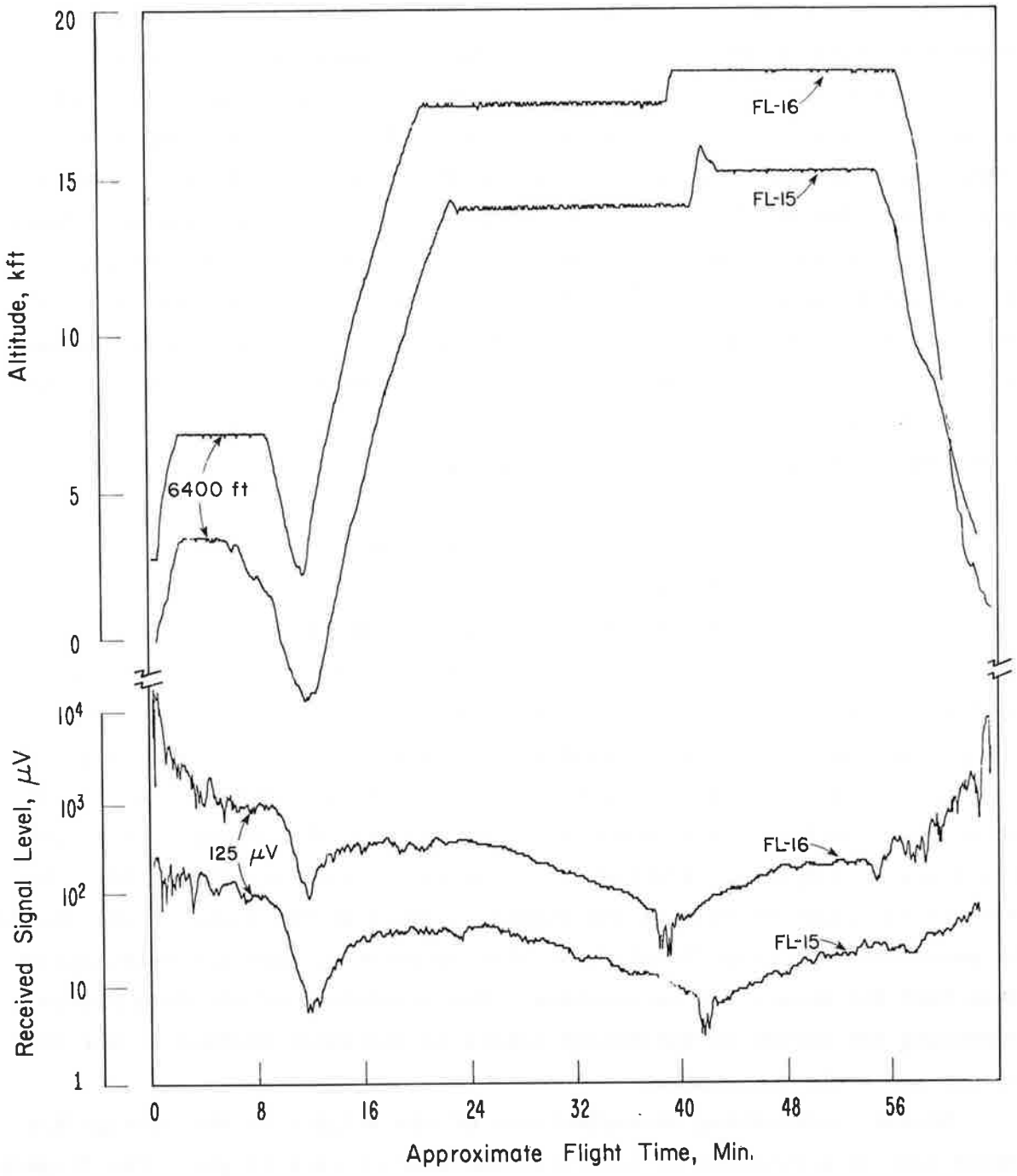

Figure 39. Example of signal repeatability for two flights over approximately the same path.

bursts, the correlation generally appears to be small. This lack of correlation is probably due, at least in part, to the 650 kHz frequency separation between the noise receiver and data link center frequency.

The measurements do, however, provide some insight into noise problems at VHF. At times, impulsive noise "spikes" 20 dB above the background noise were observed. The maximum amplitude of these spikes could not be measured due to limiting in the noise receiver. An example of the noise as a function of time is shown in figure 40. Noise units are in dB relative to the normal background noise level. Also plotted on the figure is the only bit error observed during that period. Note that the error appears to be correlated with a noise spike. However, errors are not produced with all noise spikes. Again, it should be pointed out that the noise receiver has a 110 kHz bandwidth which is much wider than a normal aircraft receiver.

4.12 Bit Error Characteristics

The bit errors exhibit a few characteristics that need to be discussed. For example, man-made noise generally causes only one or two errors in a 1 second data sample. Errors due to aircraft maneuvering, however, appear in larger bursts typically 10 to 100 bit errors per 1 second data sample. Clock slip indications are generally coincidental with error bursts greater than 30 bits and absent with error bursts less than 30 bits. Examples of these characteristics are shown in figure 41 where the number of bit errors per 1 second sample are plotted as a function of time for flight 16. The most likely cause of each of the events is noted on the figure. One should be aware than the term "bursts", in this discussion, does not necessarily mean that the errors are consecutive. The resolution of the data prevents examining the errors in sufficient detail to determine whether or not the errors are truly consecutive.

Another interesting characteristic of the flights is the average bit error rate as a function of direction and time of each flight. The flights with the highest bit error rate, as can be seen in figure 42, are the Norfolk flights at 1300 hours. This plot is for the case where the equipment, operational, and near horizon errors have been removed. The flights with the lowest average bit error rate are the Scranton flights (with the

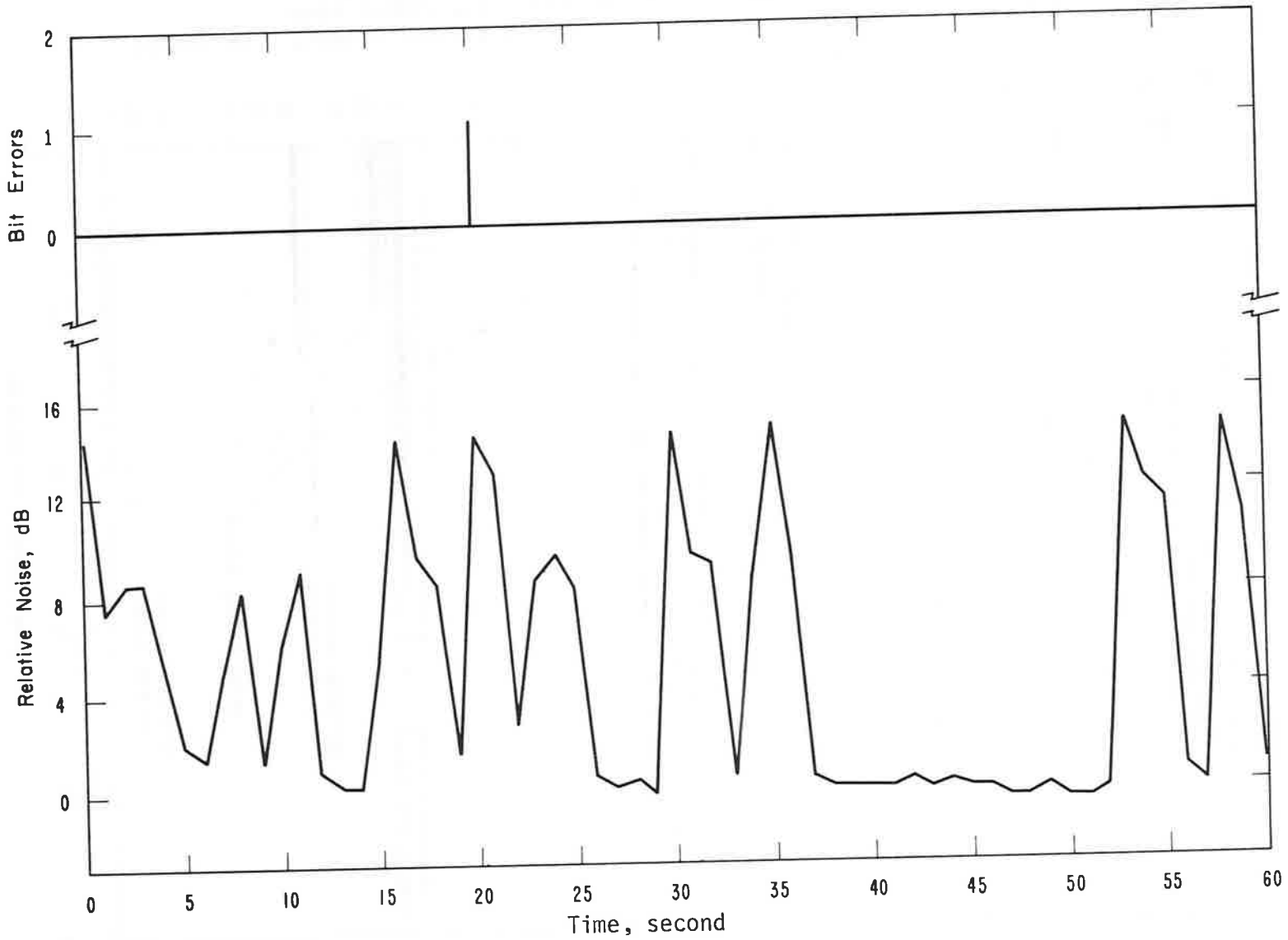

Figure 40. Sample of received noise and bit errors as a function of time.

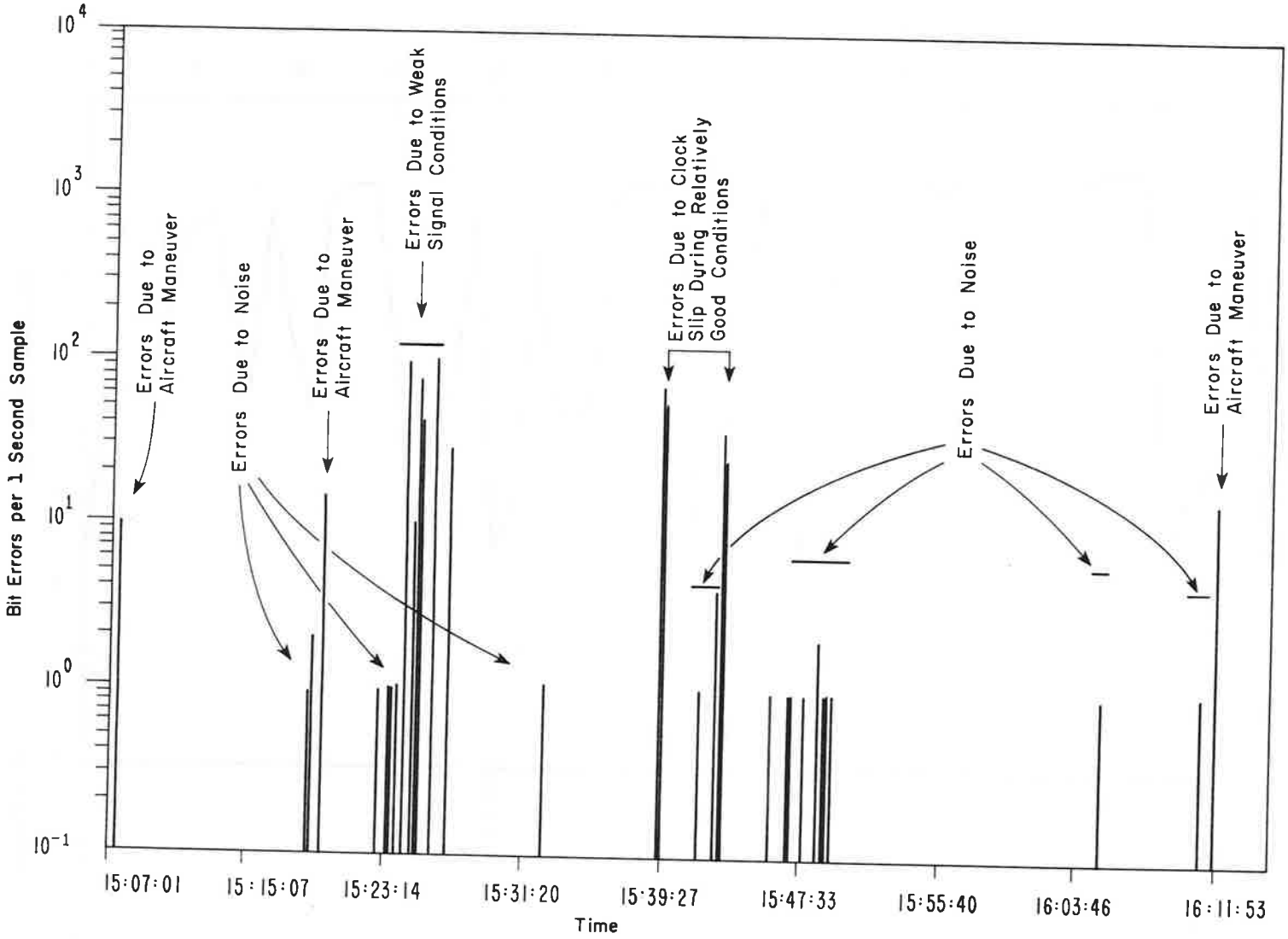

Figure 41. Example showing the characteristics of bit errors per 1 second data sample for flight 16 versus time.

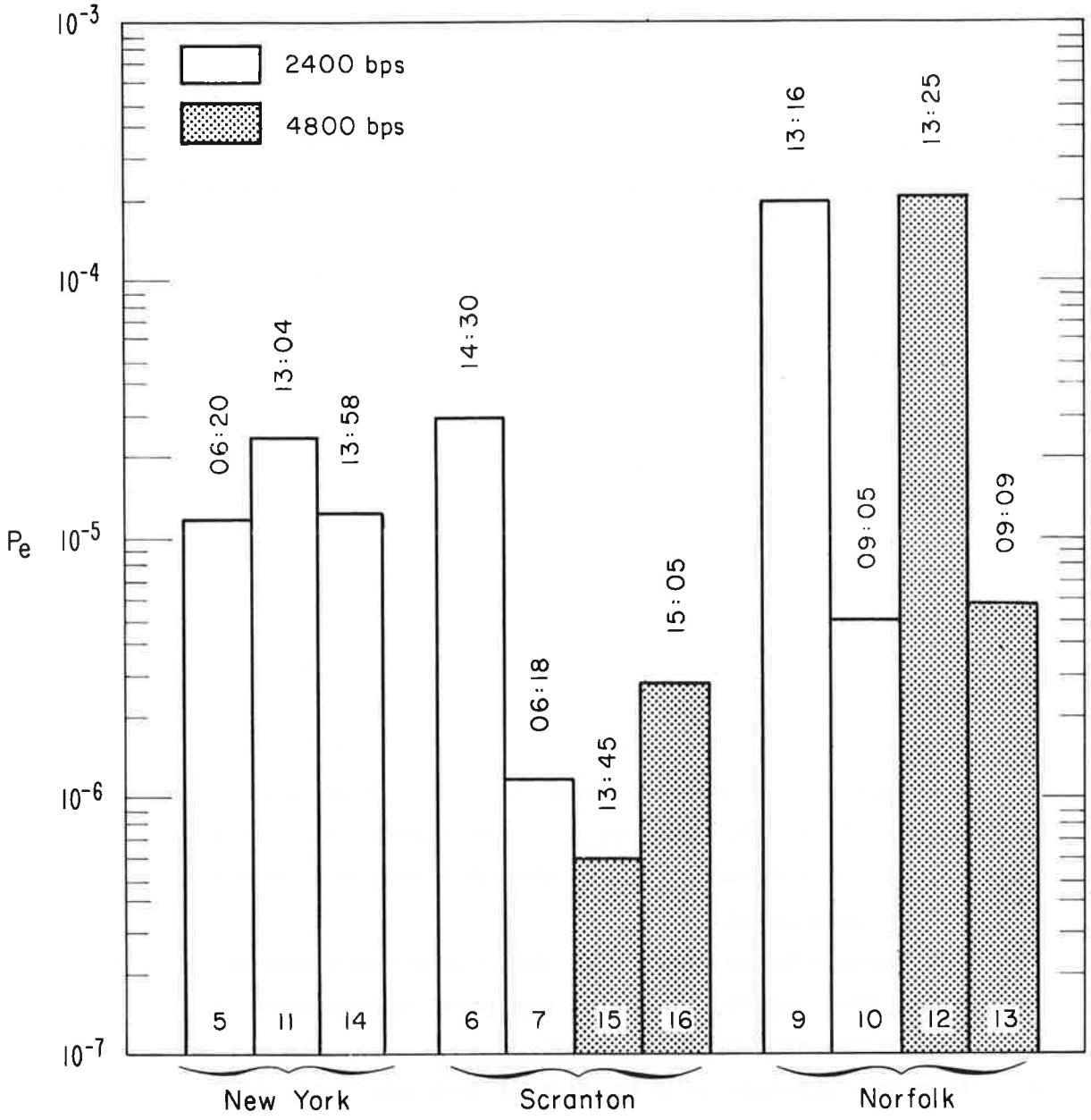

Figure 42. Average bit error rate for all flights as a function of direction and starting time of flights. Equipment, operational, and near horizon errors have been removed.

exception of flight 6). All of the New York flights are consistent in that the error rate of each of the three flights is near 10^{-5}.

5. CONCLUSIONS

A number of conclusions and observations can be made about air-to-ground digital transmission. This section will summarize these conclusions and also discuss some of the more general aspects of the tests. The conclusions are as follows:

a. The bit error rate is nearly identical for the 2400 and 4800 bps flights. This result is true even when the aircraft is near the receiving site and is probably due to the fact the performance is not limited by the noise. Thus, 4800 bps does not appear to offer any significant disadvantage in terms of poorer performance.

b. The average bit error for all flights is 4.6×10^{-5} using unweighted averaging and 6.8×10^{-5} with weighted averaging. This excludes errors due to equipment operational problems and the high error rate periods when the aircraft is near the radio horizon. The maximum and minimum average bit error rates are 2.1×10^{-4} that occurred during flight 12 and 5.6×10^{-7} that occurred during flight 15. The variation in average bit error rate is attributed to the flight path and site effects rather than noise.

c. The average block error rate for a 1000 bit block is 1.6×10^{-2}, again, excluding equipment operational errors and near horizon periods.

d. When the aircraft is 0 to 20 n mi from the site, the average bit error rate is 2.5×10^{-5}. This decreases to 6.7×10^{-6} when the aircraft is 20 to 40 n mi from the site. The increase in bit error rate when the aircraft is 0 to 20 n mi is probably due to the increase in signal fading that occurs in this region.

e. Signal fading is caused by the addition of ground reflections with the directly radiated signal. Signal variation, as observed in a 10 second period (slow fading), is substantially greater when the aircraft is close to the ground site. A maximum variation of 20 dB is observed when the aircraft is 0 to 10 n mi from the site and 8 dB for 10 to 20 n mi out. When the aircraft is 20 to 30 n mi from the site, the signal variation reduced to 6.5 dB.

f. The average received signal level samples are, on the average, equal to the theoretical calculation given in equation (4). Occasionally average signal level samples 6 dB above theoretical were measured, and are attributed to the addition of ground reflections with the direct signal.

g. The average number of error bits in a 1000 bit block, given that the block has 1 or more errors, is 2.4 bits at 2400 bps and 3.9 bits at 4800 bps. These figures showed little change with an increase in the block size to a 1 second block. No attempts were made to measure burst error characteristics other than the averages described in the preceeding.

h. Signal fading during aircraft maneuvering appears to be a complex function of the aircraft roll, pitch, and yaw relative to the receiver. Signal changes as high as 14.8 dB are observed during aircraft maneuvers. Slow aircraft maneuvers do not appear to cause any abnormal error conditions; however, sudden aircraft changes can cause errors.

i. Acquisition and ability to maintain synchronization as evidenced by clock slips and carrier loss indications largely occur during weak signal conditions. Clock slips generally are encountered during the weak signal periods when the aircraft is inbound from locations beyond the radio horizon. Evidently, the received signal has not sufficiently stabilized for proper bit synchronization during these periods.

j. A few occasions were noted where clock slips occurred during relatively good signal conditions (10 to 200 microvolts). The cause of these clock slips could not be linked with any of the recorded data. An example is shown where a burst of 90 errors occurred during one of these clock slips. Probably one of the least understood problems during the tests is where clock slips occur during relatively stable signal conditions. The phenomenon may be peculiar to the test configuration or equipment used during these flights. Thus there is a possibility that the problem can be either eliminated or reduced by sending a synchronization sequence before each message. Interference or noise is another possible cause of the problem.

k. When the aircraft approaches the radio horizon, a region of abnormally high bit error rate is encountered just prior to the loss of signal. This region is denoted in the report as the near-horizon region and probably will be unusable for data link communications. The region is encountered on the inbound as well as the outbound flights. A plot of 34 near horizon regions as a function of slant range and altitude is shown in figure 32. These measurements generally coincide with the ITS predictions for the radio horizon since 30 of the 34 samples are either partially or totally within the 5-95% confidence range. The width of the near horizon region varies between 0.5 and 21 n mi with an average of 10 n mi.

l. Measurements of average received signal level on two different flights following the same flight profile showed that the received signal level is repeatable at slant ranges greater than 30 n mi. At slant ranges less than 30 n mi, the average received signal level appears to be highly variable due to the fading and shows little correlation between the two flights over nearly the same flight path.

m. An estimate of the combined antenna gain is made in the report, based on the average received signal level. The estimate is 4 dB relative to isotropic and is the combined or total gain of both aircraft and ground antennas. Both of these antennas are approximately omnidirectional in the horizontal plane.

Modem synchronization and acquisition, in general, is a subject where additional knowledge would be beneficial. Quite possibly tradeoffs exist that would enable better synchronization and acquisition in weak or severe, fading conditions. While the problems of acquisition are not examined in this series of tests, acquisition is likely to be affected by the fading that was observed.

One additional problem will be described that does not appear in any of the measurements. Evidently, severe interference occurred when the second bottom-mounted aircraft antenna was used for VHF voice reception while the first antenna was transmitting the test signal. Possibly, the two bottom-mounted antennas do not have sufficient isolation. Thus, the second bottom antenna cannot be used for voice reception when the other is transmitting a data link signal even though the two are widely separated in frequency. The cure during these tests was to use the top-mounted antenna for voice communications and the bottom antenna for the data link.

6. REFERENCES

Bennett, W. R., and S. O. Rice (1963), Spectral density and autocorrelation functions with binary frequency-shift keying, BSTJ, September, 2355-2385.

Gierhart, G. D., and M. E. Johnson (1973), Computer programs for air/ground propagation and interference analysis (0.1 to 20 GHz), Report No. FAA-RD-73-103, AD-770335, Federal Aviation Administration, Washington, D.C., September.

Juroshek, J. R. (1973a), Compatibility measurements of digital MSK and voice transmission, Rept. No. FAA-RD-73-63, Federal Aviation Administration, Washington, D.C., April.

Juroshek, J. R. (1973b), Power spectra of computer simulated frequency modulation with digital MSK and voice input, Rept. No. FAA-RD-73-56, Federal Aviation Administration, Washington, D.C., March.

☆U.S. GOVERNMENT PRINTING OFFICE: 1976——678—961/318 REGION NO. 8